ARTICLES
https://doi.org/10.1038/s41559-022-01753-8

nature ecology & evolution

Check for updates

A polar bear paleogenome reveals extensive ancient gene flow from polar bears into brown bears

Ming-Shan Wang[1,2], Gemma G. R. Murray[3], Daniel Mann[4,5], Pamela Groves[5], Alisa O. Vershinina[2], Megan A. Supple[1,2], Joshua D. Kapp[2], Russell Corbett-Detig[6], Sarah E. Crump[2], Ian Stirling[7,8], Kristin L. Laidre[9], Michael Kunz[10], Love Dalén[11,12], Richard E. Green[6] and Beth Shapiro[1,2] ✉

Polar bears (*Ursus maritimus*) and brown bears (*Ursus arctos*) are sister species possessing distinct physiological and behavioural adaptations that evolved over the last 500,000 years. However, comparative and population genomics analyses have revealed that several extant and extinct brown bear populations have relatively recent polar bear ancestry, probably as the result of geographically localized instances of gene flow from polar bears into brown bears. Here, we generate and analyse an approximate 20X paleogenome from an approximately 100,000-year-old polar bear that reveals a massive prehistoric admixture event, which is evident in the genomes of all living brown bears. This ancient admixture event was not visible from genomic data derived from living polar bears. Like more recent events, this massive admixture event mainly involved unidirectional gene flow from polar bears into brown bears and occurred as climate changes caused overlap in the ranges of the two species. These findings highlight the complex reticulate paths that evolution can take within a regime of radically shifting climate.

Climate oscillations, such as the transitions between glacial and interglacial periods that characterized the Pleistocene, can cause species' ranges to contract, fragment or expand, as well as creating opportunities for specialization and adaptation[1]. Population genomic data reveal that climate-driven range shifts also allow admixture between closely related lineages that have not yet evolved complete reproductive isolation[2–6]. The resulting gene flow transfers both adaptive and maladaptive alleles between lineages[7–12], resulting in reticulate evolution that complicates strategies to protect endangered species and highlights the potential of admixture as an evolutionary force[5,8,13,14].

One of the best-known examples of post-divergence admixture is that between brown bears, *Ursus arctos*, and polar bears, *Ursus maritimus*. Polar bears diverged from brown bears approximately 500,000 years ago (ka)[15]. Polar bears have since evolved into a behaviourally, physiologically and morphologically distinct lineage with low genetic diversity and adaptations for life along the Arctic continental shelf[15]. In contrast, brown bears are genetically diverse and have historically occupied one of the broadest range distributions of any extant mammal[15,16]. Brown bears range from Western Europe to North America and from the Himalayas to the tundra regions of Arctic Europe and Asia. Whereas polar bears are specialized hunters of marine mammals on the sea ice, brown bears are generalized foragers within a wide range of habitats. Some brown bear populations subsist mainly on plants, while others rely on fish and/or large ungulates. Despite their distinct ecologies, polar and brown bears are not reproductively isolated and hybrid offspring have been produced both in captivity[17] and in the wild[4,15,18–20].

Previous genomic studies suggest that admixture between brown and polar bears most frequently results in introgression of polar bear DNA into brown bear genomes but not the other way around. In the ABC Islands of south-east Alaska, for example, brown bears derive 6–8% of their genomes from admixture that occurred with female polar bears during the later stages of the last ice age, perhaps between 17 and 14 ka (refs. [18,19]). Separate admixture events during the last ice age led to members of the now-extinct population of brown bears in what is now Ireland having as much as 20% polar bear ancestry[4]. Variable levels of admixture with polar bears also occurred among brown bears living on Japan's Inikari Islands[4].

In addition to this relatively recent gene flow, genomic data hint at much earlier admixture events between brown and polar bears. For example, Liu et al.[15] detected short segments of admixed polar bear DNA in European and North American brown bear genomes that they hypothesized may derive from admixture more than 150,000 ka. Because recombination reduces the size of admixed genomic segments over generations[7,21], this hypothesis has been difficult to test.

[1]Howard Hughes Medical Institute, University of California Santa Cruz, Santa Cruz, CA, USA. [2]Department of Ecology and Evolutionary Biology, University of California Santa Cruz, Santa Cruz, CA, USA. [3]Department of Veterinary Medicine, University of Cambridge, Cambridge, UK. [4]Department of Geosciences, University of Alaska, Fairbanks, AK, USA. [5]Institute of Arctic Biology, University of Alaska, Fairbanks, AK, USA. [6]Department of Biomolecular Engineering, University of California Santa Cruz, Santa Cruz, CA, USA. [7]Department of Biological Sciences, University of Alberta, Edmonton, Alberta, Canada. [8]Wildlife Research Division, Environment and Climate Change Canada Department of Biological Sciences, University of Alberta, Edmonton, Alberta, Canada. [9]Polar Science Center, Applied Physics Laboratory, University of Washington, Seattle, WA, USA. [10]University of Alaska Museum of the North, Fairbanks, AK, USA. [11]Department of Bioinformatics and Genetics, Swedish Museum of Natural History, Stockholm, Sweden. [12]Centre for Palaeogenetics, Stockholm, Sweden. ✉e-mail: beth.shapiro@gmail.com

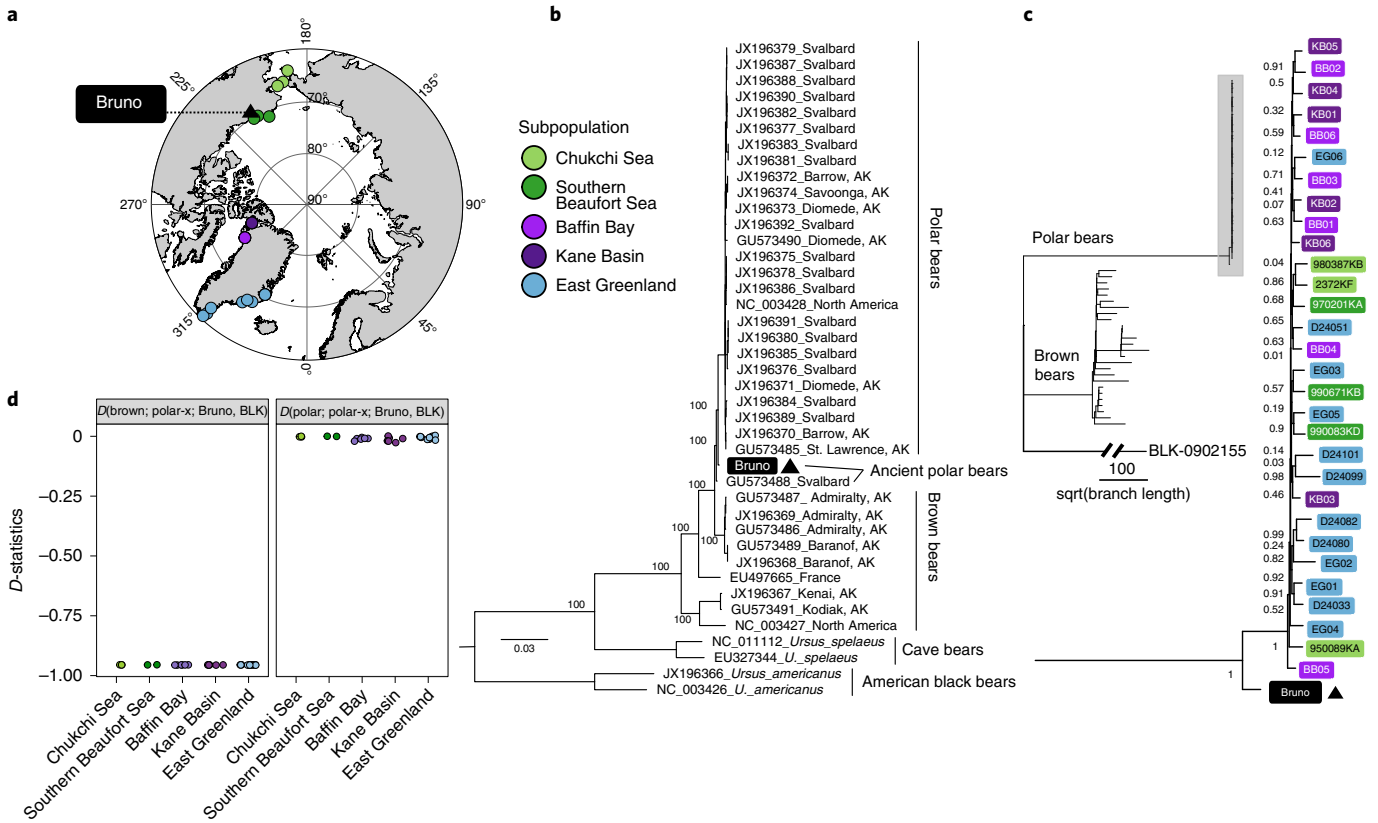

Fig. 1 | Sample location and genetic affinity of bears. a, Map describing the locations of origin for polar bear nuclear genomes analysed in this study and Bruno (black triangle). The colours indicate the subpopulation from which each polar bear genome is derived. **b**, Maximum likelihood phylogeny of 41 mitochondrial genomes from the brown, polar, cave and American black bears places Bruno (black) outside of the diversity of modern polar bears in a clade with an ancient polar bear from Svalbard, Norway, which dates to 110–130 ka (ref. [63]). **c**, A neighbour-joining tree of complete nuclear genomes using transversion sites from 26 brown bears, 30 polar bears and 1 American black bear places Bruno outside the diversity of extant polar bears. The inset shown is with the outgroup removed and branch lengths of the polar bear clade square root-transformed for improved tree rendering. Bootstrap supported the nodes below. **d**, A *D*-statistics[69,70] confirmed Bruno's basal position relative to modern polar bears. For *D*(P1, P2, P3, O), positive *D* values suggest that P3 shares more derived alleles with P1 than with P2; negative *D* values indicate that P3 shares more derived alleles with P2 than with P1. Calculations in the form of *D*(brown bear, polar bear; Bruno, BLK) yielded significant negative values (*z*-scores from all tests were −100), suggesting that Bruno shares more derived alleles with extant polar bears than with brown bears. *D*(polar bear1; polar bear-x; Bruno, BLK) was non-significant (*z*-scores from these tests ranged from −2.6 to 0.33), indicating that Bruno is not more closely related to any particular extant polar bear.

In 2009, the skull of a juvenile polar bear nicknamed 'Bruno' (now part of the collection at the University of Alaska Museum of the North, accession no. UAMES 29513) was found on the beach of the Beaufort Sea near Point McLeod in Arctic Alaska (Fig. 1a and Extended Data Fig. 1). Three radiocarbon dates on the skull yielded non-finite ages (Methods). The geomorphic setting where this skull was found (Methods) suggests that Bruno lived during the most recent period when the relative sea level was higher than today, possibly during the Pelukian Transgression between 110 and 70 ka before present when the sea was as much as 10 m higher than today along this portion of the Beaufort Sea coastline[22]. Given this potential age, Bruno's genome provides an opportunity to explore older episodes of admixture that are undetectable in genomes of more recent bears. Analysis of this ancient polar bear genome reveals evidence of a previously unrecognized admixture event between polar and brown bears. Genes from this admixture event are shared among all living brown bear populations, contributing to our inability to detect it using only genomes from extant bears.

Results

We generated a high coverage mitochondrial and 20.3-fold coverage nuclear genome using ancient DNA from the root of a tooth extracted from Bruno's skull (Methods). Using an optimized approach to recover degraded fragments of DNA[23], we prepared a total of 14 indexed libraries for sequencing. When mapped to the polar bear reference genome (GCF_017311325.1), these libraries ranged in endogenous content from 69 to 85% (Supplementary Table 1). Mapped sequences were short, with read lengths of 83 ± 34 (mean $\pm$ s.d.) base pairs (bp) (Supplementary Table 1), with excess cytosine deamination at the read ends (Extended Data Figs. 2 and 3), as is characteristic for ancient DNA[24]. The average read depth across the X chromosome was 18.6-fold, indicating that Bruno was female. We then analysed these data along with previously published mitochondrial and nuclear genomes from polar, brown and American black bears (Supplementary Tables 2 and 3) to estimate Bruno's age, infer evolutionary relationships between Bruno and extant bear populations and explore the extent of gene flow between brown and polar bears during previous intervals of potential range overlap.

Genomic data confirmed that Bruno is genetically distinct from living polar bears and, as suggested by the geological record, probably lived during the marine isotope stage (MIS) 5 interglacial period. Mitochondrial (Fig. 1b) and nuclear (Fig. 1c) phylogenies as well as *D*-statistics (Fig. 1d) place Bruno outside the diversity of

extant polar bears but within a clade that includes both extant and ancient polar bear mitogenomes.

Using our panel of polar bears, we measured the derived allele frequency spectrum. Then, we measured whether the frequency of a derived allele in extant polar bears accurately predicts its presence in extant polar bears, brown bears and in Bruno (Extended Data Fig. 4). As expected, all extant polar bears carry derived alleles as often as predicted by polar bear-derived allele frequencies. Brown bears, on the other hand, sometimes share derived allele variation in polar bears, probably because of past admixture. But the presence of a derived allele in brown bears is not well predicted by its frequency in polar bears. The rate of derived alleles found in Bruno fell between extant polar and brown bears. This is consistent with Bruno's genome existing before the time to most recent common ancestor (MRCA) of extant polar bears in many genomic regions, having a different genetic drift history or a combination of the two.

Pairwise sequentially Markovian coalescent (PSMC)[25] estimated changes in effective population size (N_e) over time revealed a divergence between Bruno's adjusted PSMC plot and that of the other polar bears approximately 110 ka (Fig. 2). Because DNA damage and low statistical power can inflate estimates of N_e in recent times[26], we extrapolated from these data and the geological context in which the skull was recovered that Bruno lived between 110 and 75 ka (Methods). This estimate is corroborated by multiple sequentially Markovian coalescent (MSMC)[27] estimates of the relative cross coalescence rate (RCCR) and divergence times between Bruno and an extant brown bear (T_1) and between extant polar bears and the same brown bear (T_2). Based on 50% RCCR, the difference in divergence time between the two pairs ($\Delta T = T_2 - T_1$), which is also an estimate of the difference in age between Bruno and living polar bears, is 104.4 ± 3.4 kyr (mean ± s.d.; Extended Data Fig. 5).

Bruno's genome provides the opportunity to explore the admixture relationship between polar and brown bears in a time window not visible using only extant genomes. *D*-statistic analysis of allele sharing between polar bears and extant brown bears shows that specific populations of brown bears have polar bear ancestry from past admixture. We recapitulate that result in this study (Extended Data Fig. 6). Replacement of the polar bear genome with Bruno's genome in the *D*-statistic analysis showed little difference in excess polar bear allele sharing between brown bears. However, *D*-statistics have no power to detect admixture that predates the population separation between brown bears.

The five-taxon D_{FOIL} (ref. [28]) approach counts the number of shared alleles based on a five-taxon symmetric phylogeny and can detect admixture at deeper nodes. Analysis of Bruno's genome revealed pervasive and strongly statistically significant admixture between the lineage leading to Bruno and the lineage leading to all extant brown bears (Fig. 3). Taken at face value, this suggests that Bruno was part of a population of polar bears that admixed into the ancestors of all brown bears, contributing genetic variation not yet found in extant polar bears. This interpretation suggests that Bruno's genome carries derived alleles that are present in all brown bears but absent from extant polar bears. A simple comparison of the number of alleles shared between Bruno, all brown bears in our panel, but absent from a polar bear confirmed this: Bruno shares more alleles with all brown bears that are also absent from another polar bear nearly twice as often as another polar bear used in this comparison (Extended Data Fig. 7).

The complex evolutionary history of brown bears, which includes episodes of admixture with polar bears and cave bears[4,15,16,18,19,29,30], may complicate the inference of admixture, in particular at deeper nodes. Therefore, we ran D_{FOIL} in several configurations (Fig. 3). First, because MSMC estimated the population divergence time for brown bears to be more recent than the death of Bruno (Extended Data Fig. 8), we ran D_{FOIL} with European and North American brown bears in positions P1 and P2 and polar bears in positions P3 and P4, with the American black bear as the outgroup (O; Fig. 3a,b). Second, we ran D_{FOIL} in a configuration in which we swapped the positions of polar and brown bears in the phylogeny (Fig. 3c,d). Although this second configuration is in contrast to our MSMC result, it is consistent with previous older estimates of the brown bear genomic MRCA[18]. Although the results presented in Fig. 3 assume a window size of 200 kilobases (kb) and exclude transitions, we recovered similar results when using window sizes spanning 100 to 500 kb, when including both transitions and transversions and assuming *P* values of 0.05, 0.01, 0.005 and 0.001 (Supplementary Figs. 1–8).

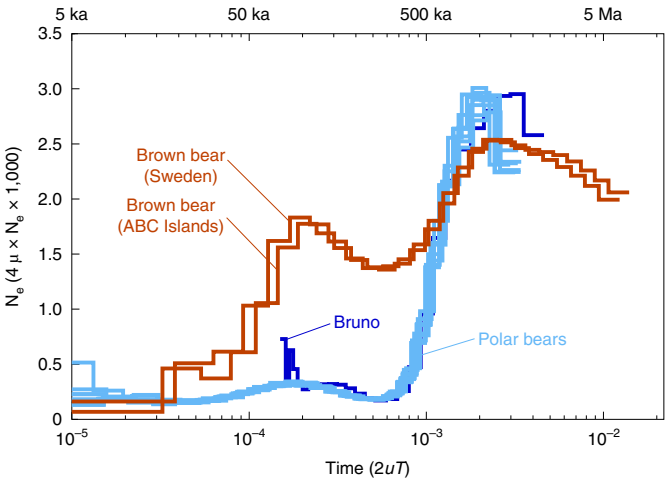

Fig. 2 | PSMC plot of effective population size over time for bears. This plot includes curves for eight polar bears from Alaska and Greenland (light blue), two brown bears (brown) from the ABC Islands (National Center for Biotechnology Information (NCBI) Sequence Read Archive (SRA) accession no. SAMN02256318) and Sweden (NCBI SRA accession no. SAMN02256313), and Bruno (dark blue). To estimate her age according to Palkopoulou et al.[68], Bruno's plot was shifted to 0.00015 (2*uT*), where her plot overlapped with those of modern polar bears. The lower *x* axis is time in units of pairwise sequence divergence per bp and the upper *x* axis is time in years scaled by a yearly mutation rate (μ) of 1×10^{-9} substitutions per site[16]. Population size on the *y* axis is given in units of $4\mu \times N_e \times 1{,}000$.

In the first configuration (Fig. 3a) and under the default *P* cut-off of 0.01, D_{FOIL} detected admixture in 10% of autosomal windows (mean ± s.d. = 1,078 ± 31 windows) and 7.4% (46 ± 5) of X chromosome windows (Fig. 3b and Supplementary Fig. 9). Most of these windows showed gene flow between Bruno's lineage and the ancestors of all extant brown bears (P4⇄P12; 79% of admixed autosomal windows and 91% of admixed X chromosome windows; Supplementary Fig. 9). This signal was confirmed by estimates of genetic divergence for admixed windows, which were lower between Bruno and brown bears than between living polar and brown bears (Supplementary Fig. 10). When we replaced Bruno as P4 with an extant polar bear, the total number of admixed windows decreased from 1,078 ± 31 to 184 ± 27 and the number of windows supporting admixture with P4 decreased from 848 ± 54 to 56 ± 9 (Fig. 3b). This confirms that the dominant admixture signal is due to specific differences between Bruno and other polar bears.

To explore how much of the admixture signal was due to Bruno's antiquity, we generated a pseudo last coalescent ancestor (LCA) of our 30 extant polar bear genomes by calling the most frequently observed allele at each locus. The LCA is expected to predominately carry the ancestral allele at sites of extant polar bear genetic variation. However, this genome will not carry derived variants in the population of polar bears that existed before extant polar bears, as Bruno does. Replacing the LCA for an extant polar bear

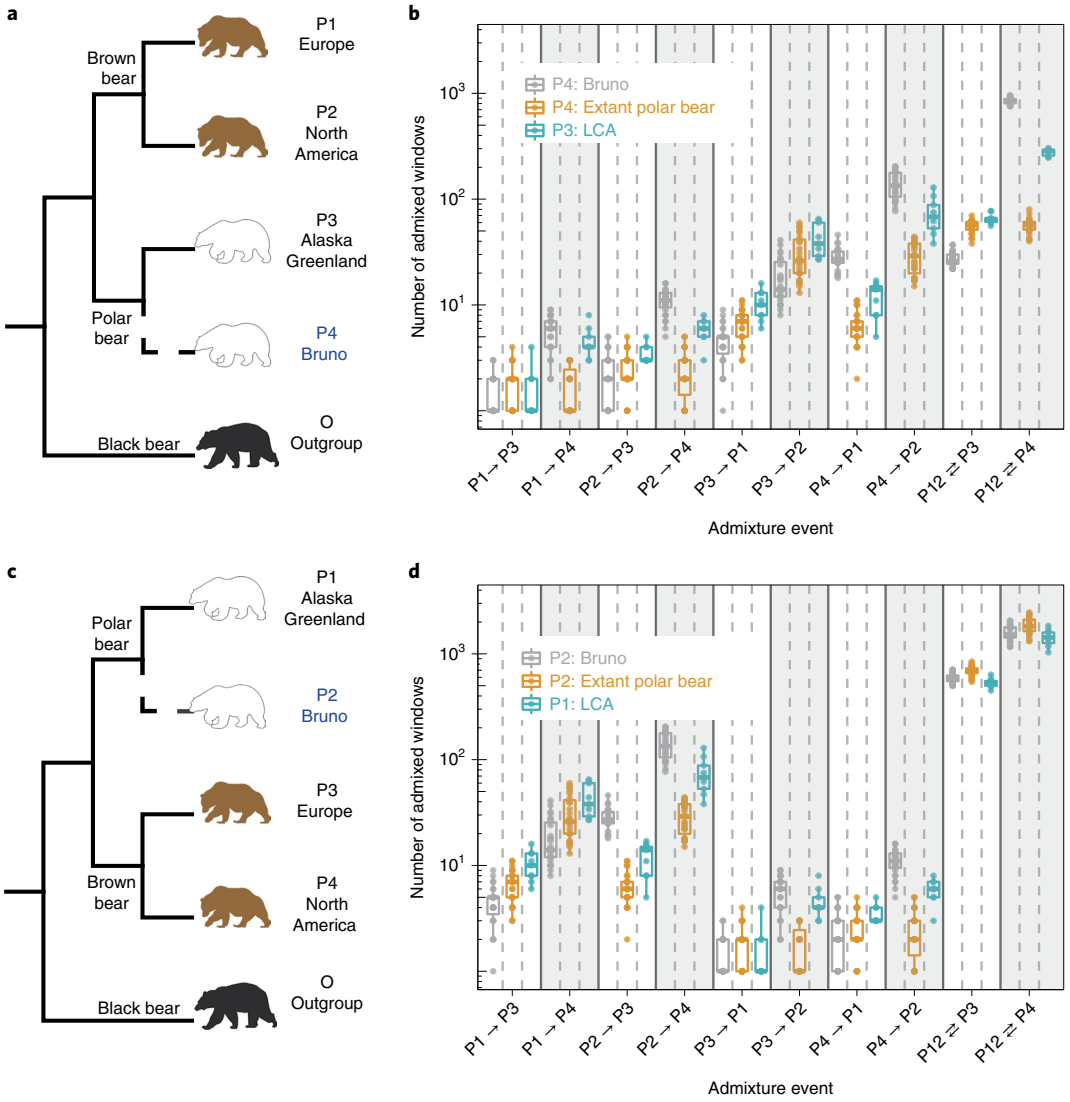

Fig. 3 | Admixture between polar and brown bears estimated using D_{FOIL}. **a**, Schematic of the topology used for the first series of D_{FOIL} analyses where the MRCA of brown bears is more recent than the MRCA of polar bears. We used three female bears for each of P1, P2 and P3. We used transversions only in 200-kb sliding windows of autosomes. **b**, Results of the D_{FOIL} analyses of independent runs ($n=3\times3\times3\times3$ when P3 represents a polar bear; $n=3\times3\times3\times1$ when P3 represents LCA) based on the schematic in **a**. We analysed a total of 11,575 autosomal 200-kb windows per run in which D_{FOIL} detected gene flow between lineages as indicated on the *x* axis. The unidirectional arrows on the *x* axis depict the direction of gene flow, while bidirectional arrows indicate that the direction of gene flow could not be distinguished. **c**, Schematic of the second topology used in D_{FOIL} analysis where the MRCA of polar bears is more recent than the MRCA of brown bears. **d**, Results of the D_{FOIL} analyses of replicated runs ($n=3\times3\times3\times3$ when P1 represents a polar bear; $n=3\times3\times3\times1$ when P1 represents LCA) based on the schematic in **c**, with arrows and box plots as in **b**. In our analysis, we used a default *P* of 0.01 by one-sided chi-squared test to retrieve potentially admixed windows. **b**,**d**, The box limit indicates the 25th and 75th percentiles of the window numbers, the centre line shows the medians, the whiskers show ±1.5 times the interquartile range, respectively. The dots indicate the number of windows with a signal of gene flow from independent runs.

in position P3 in the D_{FOIL} analysis, we found that the dominant admixture signal was between Bruno and the common ancestor of brown bears (P4⇄P12). However, the proportion of admixed windows in this category declined from 79% ($n=848\pm54$) to 57% ($n=276\pm21$) of admixed autosomal windows (Fig. 3b) and from 91% ($n=42\pm5$) to 80% ($n=14\pm3$) of admixed X chromosome windows (Supplementary Fig. 9); the number of autosomal windows supporting admixture between the LCA of polar and brown bears (P3⇄P12) increased from 2% ($n=26\pm4$) to 13% ($n=65\pm7$) (Fig. 3b).

In the second configuration (Fig. 3c), most admixed windows support gene flow between the ancestors of extant brown bears and the ancestors of both Bruno and extant polar bears, including when an extant polar bear is P2 or the LCA is P1 (Fig. 3d). This suggests that at least some of the admixture detectable with Bruno's genome may have predated the MRCA of Bruno and extant polar bears.

Intriguingly, both configurations identify gene flow from brown bears into Bruno, suggesting that gene flow occurred from brown bears into polar bears. However, gene flow from brown bears into extant polar bears is only supported when the polar bear LCA is used as P2 and fewer windows support this than support gene flow from brown bears into Bruno. This may reflect admixture from brown bears into polar bears that has largely been lost from extant polar bear genomes, which is consistent with the hypothesis that brown bear ancestry in polar bears is associated with a fitness cost[19].

That admixture is supported in both configurations indicates that the result is not impacted by model misspecification due to imprecise estimates of the timing of brown bear population divergence. Instead, the availability of Bruno's paleogenome has made it possible to detect an ancient admixture event that impacted all extant brown bears (Extended Data Fig. 9 and Supplementary Fig. 11). The antiquity of the admixture event was supported by admixture dating analysis using MSMC isolation-migration (MSMC-IM)[31], which estimated a peak duration of post-divergence gene flow between polar and brown bears around 100 ka (Fig. 4, Extended Data Fig. 10 and Supplementary Fig. 12).

While the strongest signal from D_{FOIL} and MSMC-IM was of admixture around the time that Bruno lived, we also recovered a signal of the more recent event around the Last Glacial Maximum (LGM) (Figs. 3b and 4). The pattern detected by D_{FOIL} is similar to that reported previously[4,18,19], in which admixture from polar bears is more common in North American than European brown bears: 2% of admixed windows support admixture from extant polar bears into North American brown bears; P3→P2; $n = 17 \pm 9$, while <1% support admixture from extant polar bears into European brown bears; P3→P1; $n = 4 \pm 2$ (Fig. 3b). When using the polar bear LCA as P3, the proportion of admixed windows supporting gene flow from the LCA into North American brown bears increased from 2 to 9% ($n = 42 \pm 16$ windows), suggesting that the LCA is a better model for the LGM admixing polar bear than is any sampled extant polar bear (Fig. 3b). This later admixture event was also detected by MSMC-IM, which estimated a second but much smaller peak around 40–20 ka (Fig. 4).

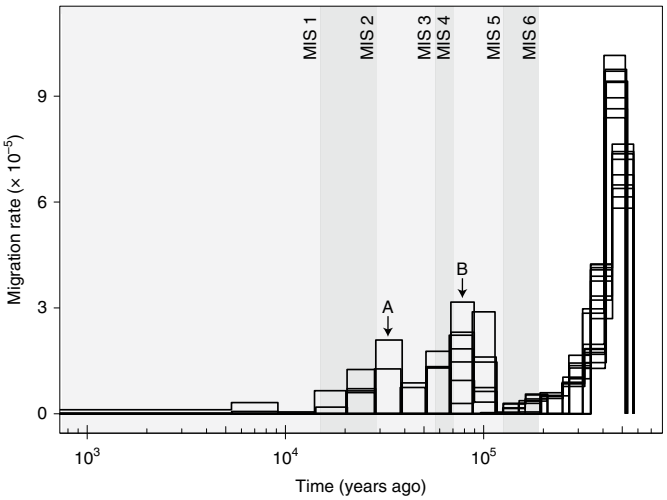

Fig. 4 | MSMC-IM analysis of gene flow between brown and polar bears over time. MSMC-IM uses coalescence rates within and across pairs of populations to fit a continuous, symmetric, isolation-migration model. The plot shows the results from 18 replicate runs, each using 2 extant polar bears and 2 extant brown bears. We identified the strongest migration peak at 400–500 ka, which corresponds to the divergence between the brown and polar bear lineages, and 2 additional peaks (A and B), which we hypothesize correspond to episodes of admixture. We note that MSMC-IM assumes symmetric migration, which may not be true for our data. However, analyses of simulated datasets showed that estimates of the timing of migration peaks are robust to the directionality of gene flow (Extended Data Fig. 10). The grey bands indicate the timing of MIS 1–6, with darker grey representing glacial periods[74]. Because precise rate estimates for brown and polar bears are not available, we used an average mutation rate for bears (family Ursidae) to scale the MSMC-IM estimation.

Discussion

Using paleogenomic data from Bruno, a polar bear that lived in northern Alaska between 110 and 75 ka, we identified an ancient episode of admixture between polar and brown bears that probably occurred during the latter substages of MIS 5, the last interglacial, when the sea ice extent in the Arctic Ocean may have been changing rapidly[32] (Fig. 4). Before the analysis of Bruno's genome, the legacy of this admixture event was undetectable in the genomes of living bears. The directionality of gene flow during this ancient admixture event was, as it also was in more recent admixture events, mostly from polar bears into brown bears (Fig. 3). However, we also found evidence of admixture from brown bears into the lineage leading to Bruno. This is consistent both with Bruno being a more recent descendent of an admixed bear and with the hypothesis, based on the absence of brown bear ancestry in living polar bears, that brown bear ancestry in polar bears is associated with a fitness cost. As revealed by the analysis of Bruno's genome, up to 10% of present-day brown bear genomes comprise ancestry that introgressed from polar bears during this ancient admixture event.

Bruno lived during 1 of the later substages of MIS 5, a period of rapid climate changes after the peak warmth of MIS 5e (129–116 ka), when temperatures warmed as much as 5–8 °C above present in Greenland and sea levels rose 6–10 m above present[33,34]. During the warm substages of MIS 5, continental ice sheets shrank, boreal forests expanded northwards and the sea ice extent was reduced in Arctic seas[32,33,35]. By analogy with the radical changes in sea ice cover and boreal ecosystems occurring today as Arctic climates warm, it is likely that Bruno lived at a time when warm conditions enabled the plant communities suitable for supporting brown bears to spread northwards to the Beaufort Sea coastline.

During the same period of warmer summers and seasonally restricted sea ice cover, polar bears may have been more abundant on shore, much as they are today with climate-induced sea ice loss. However, polar bears, which are not adapted to feed on terrestrial food sources[36], would not have to leave the coast in search of food. Instead, they could have fed on marine mammals that use terrestrial habitats for reproduction, such as walrus and other pinnipeds, as well as scavenge on whale carcasses[37]. This source of rich nutrition along the coast would also have attracted brown bears to scavenge, where they may have remained for extended periods and been in contact with polar bears, as they are in the present day[38]. Because the breeding seasons of the two species overlap roughly from late April through June[39,40], these shifts in the distributions of both brown and polar bears could have created conditions favourable to admixture over a protracted period.

In the past, polar bears also expanded their range into the southern Bering Sea and even into the North Pacific as sea ice spread during the coldest periods of the last ice age[41]. We know that at some stage, polar bears mated with brown bears because in both the Alexander Archipelago of south-east Alaska and the Kuril Islands of eastern Siberia, brown bears still carry polar bear genes. Therefore, it is likely that admixture between brown and polar bears occurred during periods of climatic transition, both glacial and interstadial conditions, and independent of absolute climate state. If repeated episodes of admixture occurred throughout their evolutionary histories, episodic hybridization may have contributed to the survival and evolutionary trajectory of both taxa. Regardless of when or how admixture happened between polar and brown bears, our results show that the large magnitude climatic shifts characteristic of Arctic regions can cause previously allopatric species to periodically commingle, creating conditions favourable for admixture.

Methods

Discovery and chronological context of Bruno's skull. We discovered the skull of a juvenile *U. maritimus* ('Bruno') (Extended Data Fig. 1) on the Beaufort Sea coast (70° 53′ 33′ N, 153° 46′ 02′ W) at Point McLeod, 9 miles west of Lonely,

Alaska. The skull's excellent preservation at a location where polar bears live today suggested that this animal died recently. However, three AMS ^{14}C dates obtained on ultrafiltered collagen extractions of bone all yielded non-finite ages (Beta-283240: >43,500 ^{14}C; OxA-23894: >50,500 ^{14}C; OxA-23986: >50,500 ^{14}C). The skull is housed at the University of Alaska Museum (UAMES 29513). Based on its non-finite age and excellent preservation, we infer that Bruno's skull was probably frozen in permafrost since death. This is consistent with its discovery on the seawards face of a coarse clastic barrier beach that is advancing shorewards across the basin of a drained thaw lake and reworking the underlying sediment as it goes.

The Beaufort Sea coastline has experienced multiple fluctuations in relative sea level (RSL) over the last several million years[42]. As a result, a series of offlapping beach ridge complexes cover the coastal plain that borders the Beaufort Sea. These beach ridge complexes consist of barrier beaches, spits and barrier islands formed when RSL was higher than today. The youngest and best-preserved of these ancient shoreline deposits dates to the Pelukian Transgression, which occurred between 110 and 70 ka during the later substages of MIS 5, the last interglacial[22]. The RSL during the Pelukian Transgression rose 6–10 m above present sea level.

We can infer a possible chronostratigraphic context for Bruno's skull by placing it into context with the RSL history of the area where it was found. When the sea transgresses across the coastal plain, it thaws the underlying permafrost and erodes the surficial sediment, reworking this and organic remains preserved there into sand and gravel barrier beaches. Ancient driftwood, bivalve shells and the battered bones of marine and terrestrial mammals occur today in the barrier beaches deposited by the Pelukian Transgression. If Bruno had died before the Transgression, her skull would probably have been transported inland by waves as the RSL rose and been battered in the process. If, alternatively, Bruno died after the Transgression when the RSL was lower than today and her skull deposited below present sea level, the surrounding sediment would have remained unfrozen and bone preservation would be poor. We speculate instead that Bruno died on sea ice several kilometres from the contemporary shoreline, either during the height or waning stages of the Transgression, at a time when the RSL was higher than today. Her skull was then deposited in subtidal muds at an altitude slightly above present-day sea level. As the RSL fell, the skull and surrounding sediment were incorporated into permafrost, remaining there until recent coastal erosion exhumed it.

Bruno's genome: data generation. We performed all pre-amplification steps in DNA extraction and library preparation pipelines in the dedicated ancient DNA processing facility at the University of California, Santa Cruz (UCSC) Paleogenomics Lab using sterile protocols developed for ancient DNA. We extracted a tooth from Bruno's skull and removed, using a Dremel tool, a fragment of the root. We powdered the root using an MM 400 Mixer Mill (Retsch) and performed 6 DNA extractions from 100–120 mg of powder. We treated 1 of 6 powder aliquots (JK578) with 0.5% sodium hypochlorite solution[43] before DNA extraction. For all 6 aliquots, we extracted DNA, following[44] with a final elution of 50 µl EBT buffer (10 mM Tris, 0.05% Tween 20).

For the DNA extracts JK300, JK578, JK579 and JK580, we prepared double-stranded DNA libraries[45] to which we added indices on both ends[46]. We prepared 50 µl reactions containing 10 µl non-indexed library, 1X AmpliTaq Gold Buffer, 2.5 mM $MgCl_2$, 0.25 mM deoxyribonucleotide triphosphates, 0.4 µM i7 indexing primer, 0.4 µM i5 indexing primer and 0.04 U µl^{-1} AmpliTaq Gold Hot Start Polymerase (Applied Biosystems). We amplified libraries using a Bio-Rad T100 thermal cycler as follows: 94° C for 10 m, followed by 25 cycles of 94° C for 30 s, 60° C for 30 s and 72° C for 40 s, followed by 72° C for 7 m.

For the DNA extracts BAN036 and BAN037, we prepared single-stranded DNA (ssDNA) libraries[23] with the following modifications: a final reaction volume of 80 µl; a 2:1 ratio of splinter:adaptor oligonucleotide; a 6:1 molar ratio of adaptor:ssDNA; and a 65:1 molar ratio of extreme thermostable single-stranded DNA binding protein:ssDNA. We double-indexed and amplified these libraries as above and prepared 50 µl reactions containing 10 µl pre-amplified library, 1X AmpliTaq Gold 360 Master Mix (Applied Biosystems), 1 µM i7 indexing primer and 1 µM i5 indexing primer. We amplified libraries as above: 95° C for 10 m, followed by 20 cycles of 95° C for 30 s, 60° C for 30 s and 72° C for 60 s, followed by 72° C for 7 m.

We purified all amplified libraries using 75 µl (1.5X) of a SPRI bead mixture[47]. We quantified the amplified libraries using a Qubit 4 (Invitrogen) and Qubit 1X dsDNA HS Assay Kit (Invitrogen). Finally, we visualized the amplified libraries on a TapeStation 2200 (Agilent Technologies) using the D1000 High Sensitivity ScreenTape Assay (Agilent Technologies).

To assess library quality, we sequenced each library to a depth of 100,000–500,000 reads at UCSC using 2×100 and 2×150 (150 cycles) chemistry for either the Illumina MiSeq or Illumina NextSeq systems. After preliminary assessments of library quality, we pooled the libraries for sequencing on an Illumina HiSeq 4000 and Xten systems located at the University of California, San Francisco CAT Core, Fulgent Genetics or SciLifeLab using 2×100 and/or 2×150 chemistry.

Bruno's genome: data processing. We used SeqPrep2 (https://github.com/jeizenga/SeqPrep2) to trim adaptors and merge paired reads with the options -o 15 -q 15. We discarded merged reads shorter than 25 bp and low-complexity reads from the downstream analysis. Details of each library are provided in Supplementary Table 1. We mapped merged reads passing quality filtration against the polar bear reference genome (GenBank accession no. GCF_017311325.1) using the Burrows–Wheeler Aligner v.0.7.12-r1039 (ref. [48]) with disabled seed option (-l 1024). We removed duplicate reads using the rmdup tool in SAMtools v.0.1.19 (ref. [49]). We used mapDamage v.2.0.6-2-g6507525 (ref. [50]) to estimate DNA fragment length distribution, measure cytosine deamination and rescale the quality of mapped reads. Approximately 7% of the first position in each read exhibited C-T or G-A substitution (Extended Data Fig. 2). We filtered the resulting BAM alignment with a minimum mapping quality of 30 and minimum read length of 35 bp using SAMtools v.0.1.19 (ref. [49]). We used snpAD v.0.3.4 (ref. [51]) to estimate the sequencing error rate and reference bias for each scaffold with the options -B -c 6. We called bases using snpADCall in snpAD, considering reference bias and sequencing error with the options -B -e –p, and removed bases with a read depth lower than one-third (--min-meanDP 7) and higher than twice (--max-meanDP 42) the average sequencing depth, and genotype quality lower than 40 (--minQ 40) using VCFtools v.0.1.5 (https://vcftools.github.io/index.html). Our final assembly had an average sequencing coverage of 20.3-fold (Supplementary Table 2).

To assemble a mitochondrial genome, we used mapping-iterative-assembler v.1.0 (ref. [52]) using the polar bear mitochondrial genome (accession no. NC_003428.1) as seed with the ancient DNA substitution matrix. We called bases with a minimum sequence depth >20X and 90% consensus, resulting in a mitochondrial genome assembly with an average read depth of 863-fold.

Other bear genomes. We downloaded data from 26 extant brown bears (18 from Europe and 8 from North America), 30 extant polar bears and 1 American black bear (Supplementary Table 2) and remapped these to the polar bear reference genome. All polar bears and 17 brown bears (9 from Europe and 8 from North America) had a genome sequencing coverage >15-fold.

We trimmed low-quality data using Trimmomatic v.0.39 (ref. [53]) with the settings -threads 10 LEADING:3 TRAILING:3 SLIDINGWINDOW:4:15 MINLEN:36. Reads passing the filter were then aligned onto the polar bear reference genome using Burrows–Wheeler Aligner-MEM v.0.7.12-r1039 (ref. [54]) with default parameters except for the -t 12 option. We sorted the alignment and removed duplicate reads using the SortSam and MarkDuplicates functions in Picard v.2.20.0-SNAPSHOT (https://github.com/broadinstitute/picard/). We called variants jointly using HaplotypeCaller from the GATK package v.3.7.0 (ref. [55]) with the --min_base_quality_score 18 option. We filtered low-quality bases using VariantFiltration from GATK with the settings QUAL < 40.0 MQ < 25.0 MQ0 ≥ 4 && ((MQ0/(1.0*DP)) > 0.1 -cluster 3 -window 10. The resulting genotype file was merged with that for Bruno using the merge function in BCFtools v.1.4-7-g41827a3-dirty (https://samtools.github.io/bcftools/). We retained biallelic alleles for subsequent analysis.

Phylogenetic inference. We generated a nuclear phylogeny using only transversion sites (to reduce the potential error introduced by ancient DNA damage) using a dataset comprising Bruno, 30 modern polar bears, 26 brown bears and 1 American black bear. We constructed a neighbour-joining tree using megacc[56] in MEGA7 (ref. [57]), with 1,000 bootstraps. The tree and accompanying map (Fig. 1a) were edited with the R (https://www.r-project.org/) packages ggplot2 v.3.3.5 (https://cran.r-project.org/web/packages/ggplot2/index.html), PlotSvalbard v.0.9.2[58], ggtree v.3.2.1[59–61] and treeio v.1.18.1[62].

To place Bruno within a mitochondrial phylogeny, we downloaded 40 published mitochondrial genomes (Supplementary Table 3), including 2 American black bears, 2 cave bears, 9 brown bears, 26 polar bears and a 120,000-year-old polar bear from Svalbard[63]. We aligned these along with Bruno using MUSCLE v.3.8.31 (ref. [64]) with default parameters, excluding the control region. We used RAxML v.8.1.17 (ref. [65]) with one partition and the GTRGAMMAI model of nucleotide evolution to construct a maximum likelihood phylogeny. We performed 1,000 bootstrap replicates and visualized the phylogeny with Figtree v.1.3.1 (https://github.com/rambaut/figtree/).

MSMC and MSMC-IM analyses. We used MSMC[27] to estimate the timing of divergence between brown and polar bears, restricting our analysis to genomes with >20-fold coverage. We used BEAGLE v.4.1 (ref. [66]) with default settings to phase the genotypes. To avoid erroneous read mapping, we generated a mappability mask file for the polar bear reference genome using the SNPable toolkit (http://lh3lh3.users.sourceforge.net/snpable.shtml) with the settings $k = 35$ and $r = 0.9$. We restricted the genome to regions with more than average but less than twice the average depth of sequencing coverage in the reference genome using SAMtools and bamCaller.py scripts from the MSMC toolkit (https://github.com/stschiff/msmc-tools). We generated the MSMC input using the generate_multihetsep.py from the MSMC toolkit. Because we sequenced only one ancient genome, we ran MSMC2 to estimate the RCCR for haplotype-phased genomes from Bruno and one of two brown bears (SAMN07422272 or SAMN07422262) and between an extant polar bear (SAMN02261853 or SAMN02261826) and the same two brown bears. We performed separate runs for the 2 different polar and brown bear pairs (Extended Data Fig. 5), with 30 bootstrap replicates. We assumed a mutation rate of 1.0×10^{-9} site per year[16] and a generation time of 11.5 years to scale to calendar years. We note that a recent ancient genome study estimated that the nuclear

substitution rate for bears was 9.56×10^{-10} substitution per site per year[29], which is similar to the rate from Kumar et al.[16].

We estimated the rate of gene flow between polar and brown bears over time using MSMC-IM[31], which uses estimates of coalescence rates within and across pairs of populations to fit a continuous isolation-migration model and estimate time-dependent rates of gene flow. We estimated coalescence rates within and across pairs of brown and polar bear populations using MSMC2 based on eight haplotypes (two brown bear genomes and two polar bear genomes). Using these estimates as input, we then ran MSMC-IM using the option -mu 1.15e-8 -beta b1,b2. As the chosen values for each pair of b1 and b2 (the -beta option) impact fit, we used a combination of values in which b1 was either 1×10^{-9}, 1×10^{-8}, 1×10^{-7}, 1×10^{-6} or 1×10^{-5}, and b2 was either 1×10^{-3}, 1×10^{-2} or 0.1, resulting in a total of 15 (5×3) b1–b2 combination pairs. We performed MSMC-IM with each pair of b1–b2 values independently and manually checked the fit. We found that the inference when using b1 as 1×10^{-8} and b2 as 1×10^{-2} better approximated the MSMC-inferred coalescence rate (Supplementary Fig. 12).

We analysed the simulated datasets to test whether the directionality of gene flow affected the MSMC-IM estimates. To generate datasets that reflected the presumed evolutionary history of brown and polar bears, we simulated evolution using msprime[67] under the scenario in which two populations (pop0 and pop1; Extended Data Fig. 10) diverged 500 ka with symmetric and asymmetric gene flow at 100 ka. We tested 8 models: 2 in which the two populations exchange 5 or 10% ancestry symmetrically and 6 in which 1 population contributes 5 or 10% ancestry to the other asymmetrically. For each model, we simulated sequences for 4 diploid individuals (corresponding to 8 haplotypes) with 30 chromosomes of length 30 Mb. We ran MSMC2 using these eight haplotypes as above and used the resulting output as input for MSMC-IM. For each model, we performed ten independent tests. MSMC-IM recovered similar results for the eight simulated datasets, suggesting that MSMC-IM estimates are robust to the directionality of gene flow (Extended Data Fig. 10).

PSMC inference of demographic history. We applied the PSMC v.0.6.5-r67 (ref. [25]) approach to infer plots of effective population size over time for Bruno, eight polar bears (SAMN02261865, SAMN02261845, SAMN02261868, SAMN02261854, SAMN02261878, SAMN19922664, SAMN19922660 and SAMN16454145) and two brown bears (SAMN02256313 and SAMN02256318). We restricted this analysis to genomes with >20-fold coverage. We generated consensus sequences containing heterozygotes for each of the 36 autosomal scaffolds with length >1 Mb using the mpileup function (-C50) of SAMtools v.0.1.18 and available scripts from the PSMC package. We required a sequencing depth for each locus above one-third of the average coverage ('-d' option) and less than twice the average coverage (-D option) and consensus quality >20. We ran PSMC with the settings -N25 -t15 -r5 -p 4+25*2+4+6, using the same mutation rate and generation time as above to scale estimations.

Because ancient genomes stop accumulating mutations at the time of death, they will contain fewer mutations (branch shortening) compared to modern genomes. To plot PSMC estimates for Bruno and the modern bear on the same calendar timescale, we used a previously described method[26,68], in which we shifted Bruno's PSMC plot along the x axis in units of divergence ($d=2uT$), using the script psmc_plot.pl from the PSMC package, until Bruno's demographic history aligned with that of modern polar bears. T represents the divergence time and u indicates the yearly mutation rate. We found that the PSMC curves for Bruno and modern polar bears overlapped when $d=0.00015$.

Admixture analysis using *D*-statistics and D_{FOIL}. To estimate allele sharing between Bruno, extant polar bears and extant brown bears, we first calculated the *D*-statistics[69] using qpDstat from AdmixTools v.6.0[70]. We measured the significance of each test using a block jackknife with $|Z|>3$ suggesting admixture. We note that qpDstat reports minimum and maximum z-scores of −100 and 100. To avoid the potential bias from ancient DNA damage, we restricted our analyses to transversion sites.

We used D_{FOIL}[28] to measure admixture among bear lineages. D_{FOIL} detects admixture based on a five-taxon phylogeny (((P1,P2),(P3,P4)),O), with the ingroup taxa arranged in two sub-pairs (P1/P2 and P3/P4), in which P1 and P2 have diverged more recently than P3 and P4, and an outgroup taxon (O). We ran D_{FOIL} in several configurations in which P1, P2, P3 and P4 are brown and polar bears and O is an American black bear. Since genetic diversity among bears is low and we restricted our analyses to transversions, we ran D_{FOIL} in 200 kb non-overlapping sliding windows across the whole genome[71] with other default parameters. For each computation, one genome was used to represent each of P1, P2, P3 and P4. For most analyses (excluding those using Bruno or the LCA of extant polar bears), we selected three genomes for each of P1, P2 and P3, resulting in a total of 27 ($3\times3\times3$) combinations. For each test, we applied the default significance cut-off of $P<0.01$ measured with the chi-squared test. To test the robustness of this analysis, we analysed transversions and all variants (transversions + transitions) separately using window sizes of 100, 150, 200, 250, 300, 350, 400 and 500 kb and with P value cut-offs of 0.05, 0.01, 0.005 and 0.001, respectively (Supplementary Figs. 1–8).

Assessing the impact of admixture on PSMC plots. Because admixture can lead to overestimation of effective population size in PSMC[25], we explored the impact of admixture from polar bears on coalescent-based estimates of effective population size over time in brown bears. We used IBDmix[72] to identify regions of brown bear genomes that are introgressed from polar bears. We set Bruno as the source (-a) and all brown bears as the admixed population, with other parameters as default, and recovered genomic regions with a length >30 kb and single-point log odds ratio score > 4 as admixed (Extended Data Fig. 9). This analysis identified more admixed segments in North American brown bears (195–378 Mb) than in European brown bears (30–127 Mb). We note that this analysis will have the most power to detect longer admixed segments not broken down by recombination.

Next, we estimated PSMC plots for two ABC Islands brown bears (SAMN02256318 and SAMN02256320) after masking these admixed regions. We removed the IBDmix-identified admixed regions from each brown bear genome (378 Mb for SAMN02256320 and 338 Mb for SAMN02256318) using the complement function of BEDTools v.2.25.0 (ref. [73]). The remaining regions were used as input for SAMtools mpileup (the -l option) to generate a diploid consensus genome sequence. As a control, randomly selected and masked 30 kb non-overlapping regions from across the genome were used, generating a dataset for each brown bear that was the same total length as the admixture-masked genomes. We ran PSMC as above. PSMC plots comparing non-masked, admixture-masked and randomly masked datasets are presented in Supplementary Fig. 11.

Reporting Summary. Further information on research design is available in the Nature Research Reporting Summary linked to this article.

Data availability

Raw reads generated from Bruno are available from the NCBI SRA BioProject accession no. PRJNA720153. Other data used are listed in Supplementary Tables 2 and 3.

Code availability

Scripts and codes for genome analysis can be accessed at https://github.com/PopGenomics-WMS/Bruno_aDNA_analysis.

Received: 27 August 2021; Accepted: 30 March 2022;
Published online: 16 June 2022

References

1. Hewitt, G. The genetic legacy of the Quaternary ice ages. *Nature* **405**, 907–913 (2000).
2. Muhlfeld, C. C. et al. Invasive hybridization in a threatened species is accelerated by climate change. *Nat. Clim. Change* **4**, 620–624 (2014).
3. Taylor, S. A. et al. Climate-mediated movement of an avian hybrid zone. *Curr. Biol.* **24**, 671–676 (2014).
4. Cahill, J. A. et al. Genomic evidence of widespread admixture from polar bears into brown bears during the last ice age. *Mol. Biol. Evol.* **35**, 1120–1129 (2018).
5. Mao, Y., Economo, E. P. & Satoh, N. The roles of introgression and climate change in the rise to dominance of *Acropora* corals. *Curr. Biol.* **28**, 3373–3382.e5 (2018).
6. Vianna, J. A. et al. Genome-wide analyses reveal drivers of penguin diversification. *Proc. Natl Acad. Sci. USA* **117**, 22303–22310 (2020).
7. Racimo, F., Sankararaman, S., Nielsen, R. & Huerta-Sánchez, E. Evidence for archaic adaptive introgression in humans. *Nat. Rev. Genet.* **16**, 359–371 (2015).
8. McKelvey, K. S. et al. Patterns of hybridization among cutthroat trout and rainbow trout in northern Rocky Mountain streams. *Ecol. Evol.* **6**, 688–706 (2016).
9. Kim, B. Y., Huber, C. D. & Lohmueller, K. E. Deleterious variation shapes the genomic landscape of introgression. *PLoS Genet.* **14**, e1007741 (2018).
10. Wu, D.-D. et al. Pervasive introgression facilitated domestication and adaptation in the *Bos* species complex. *Nat. Ecol. Evol.* **2**, 1139–1145 (2018).
11. Wang, M.-S. et al. Ancient hybridization with an unknown population facilitated high-altitude adaptation of canids. *Mol. Biol. Evol.* **37**, 2616–2629 (2020).
12. Meier, J. I. et al. Ancient hybridization fuels rapid cichlid fish adaptive radiations. *Nat. Commun.* **8**, 14363 (2017).
13. Haig, S. M., Mullins, T. D., Forsman, E. D., Trail, P. W. & Wennerberg, L. I. V. Genetic identification of spotted owls, barred owls, and their hybrids: legal implications of hybrid identity. *Conserv. Biol.* **18**, 1347–1357 (2004).
14. vonHoldt, B. M. et al. Whole-genome sequence analysis shows that two endemic species of North American wolf are admixtures of the coyote and gray wolf. *Sci. Adv.* **2**, e1501714 (2016).
15. Liu, S. et al. Population genomics reveal recent speciation and rapid evolutionary adaptation in polar bears. *Cell* **157**, 785–794 (2014).
16. Kumar, V. et al. The evolutionary history of bears is characterized by gene flow across species. *Sci. Rep.* **7**, 46487 (2017).

17. Preuß, A., Ganslosser, U., Purschke, G. & Magiera, U. Bear-hybrids: behaviour and phenotype. *Zool. Gart.* **78**, 204–220 (2009).
18. Cahill, J. A. et al. Genomic evidence for island population conversion resolves conflicting theories of polar bear evolution. *PLoS Genet.* **9**, e1003345 (2013).
19. Cahill, J. A. et al. Genomic evidence of geographically widespread effect of gene flow from polar bears into brown bears. *Mol. Ecol.* **24**, 1205–1217 (2015).
20. Pongracz, J. D., Paetkau, D., Branigan, M. & Richardson, E. Recent hybridization between a polar bear and grizzly bears in the Canadian Arctic. *Arctic* **70**, 151–160 (2017).
21. Pugach, I., Matveyev, R., Wollstein, A., Kayser, M. & Stoneking, M. Dating the age of admixture via wavelet transform analysis of genome-wide data. *Genome Biol.* **12**, R19 (2011).
22. Farquharson, L. et al. Alaskan marine transgressions record out-of-phase Arctic Ocean glaciation during the last interglacial. *Geology* **46**, 783–786 (2018).
23. Kapp, J. D., Green, R. E. & Shapiro, B. A fast and efficient single-stranded genomic library preparation method optimized for ancient DNA. *J. Hered.* **112**, 241–249 (2021).
24. Briggs, A. W. et al. Patterns of damage in genomic DNA sequences from a Neandertal. *Proc. Natl Acad. Sci. USA* **104**, 14616–14621 (2007).
25. Li, H. & Durbin, R. Inference of human population history from individual whole-genome sequences. *Nature* **475**, 493–496 (2011).
26. Fu, Q. et al. Genome sequence of a 45,000-year-old modern human from western Siberia. *Nature* **514**, 445–449 (2014).
27. Schiffels, S. & Durbin, R. Inferring human population size and separation history from multiple genome sequences. *Nat. Genet.* **46**, 919–925 (2014).
28. Pease, J. B. & Hahn, M. W. Detection and polarization of introgression in a five-taxon phylogeny. *Syst. Biol.* **64**, 651–662 (2015).
29. Barlow, A. et al. Middle Pleistocene genome calibrates a revised evolutionary history of extinct cave bears. *Curr. Biol.* **31**, 1771–1779.e7 (2021).
30. Barlow, A. et al. Partial genomic survival of cave bears in living brown bears. *Nat. Ecol. Evol.* **2**, 1563–1570 (2018).
31. Wang, K., Mathieson, I., O'Connell, J. & Schiffels, S. Tracking human population structure through time from whole genome sequences. *PLoS Genet.* **16**, e1008552 (2020).
32. Polyak, L. et al. History of sea ice in the Arctic. *Quat. Sci. Rev.* **29**, 1757–1778 (2010).
33. Dutton, A. et al. Sea-level rise due to polar ice-sheet mass loss during past warm periods. *Science* **349**, aaa4019 (2015).
34. Salonen, J. S. et al. Abrupt high-latitude climate events and decoupled seasonal trends during the Eemian. *Nat. Commun.* **9**, 2851 (2018).
35. Guarino, M.-V. et al. Sea-ice-free Arctic during the Last Interglacial supports fast future loss. *Nat. Clim. Change* **10**, 928–932 (2020).
36. Rode, K. D., Robbins, C. T., Nelson, L. & Amstrup, S. C. Can polar bears use terrestrial foods to offset lost ice-based hunting opportunities? *Front. Ecol. Environ.* **13**, 138–145 (2015).
37. Laidre, K. L., Stirling, I., Estes, J. A., Kochnev, A. & Roberts, J. Historical and potential future importance of large whales as food for polar bears. *Front. Ecol. Environ.* **16**, 515–524 (2018).
38. Miller, S., Wilder, J. & Wilson, R. R. Polar bear–grizzly bear interactions during the autumn open-water period in Alaska. *J. Mammal.* **96**, 1317–1325 (2015).
39. Steyaert, S. M. J. G., Endrestøl, A., Hackländer, K., Swenson, J. E. & Zedrosser, A. The mating system of the brown bear *Ursus arctos*. *Mamm. Rev.* **42**, 12–34 (2012).
40. Stirling, I., Spencer, C. & Andriashek, D. Behavior and activity budgets of wild breeding polar bears (*Ursus maritimus*). *Mar. Mamm. Sci.* **32**, 13–37 (2016).
41. Méheust, M., Stein, R., Fahl, K. & Gersonde, R. Sea-ice variability in the subarctic North Pacific and adjacent Bering Sea during the past 25 ka: new insights from IP_{25} and $U^{k'}_{37}$ proxy records. *Arktos* **4**, 1–19 (2018).
42. Brigham-Grette, J. & Hopkins, D. M. Emergent marine record and paleoclimate of the last interglaciation along the northwest Alaskan coast. *Quat. Res.* **43**, 159–173 (1995).
43. Boessenkool, S. et al. Combining bleach and mild predigestion improves ancient DNA recovery from bones. *Mol. Ecol. Resour.* **17**, 742–751 (2017).
44. Dabney, J. et al. Complete mitochondrial genome sequence of a Middle Pleistocene cave bear reconstructed from ultrashort DNA fragments. *Proc. Natl Acad. Sci. USA* **110**, 15758–15763 (2013).
45. Meyer, M. & Kircher, M. Illumina sequencing library preparation for highly multiplexed target capture and sequencing. *Cold Spring Harb. Protoc.* **2010**, pdb.prot5448 (2010).
46. Kircher, M., Sawyer, S. & Meyer, M. Double indexing overcomes inaccuracies in multiplex sequencing on the Illumina platform. *Nucleic Acids Res.* **40**, e3 (2012).
47. Rohland, N. & Reich, D. Cost-effective, high-throughput DNA sequencing libraries for multiplexed target capture. *Genome Res.* **22**, 939–946 (2012).
48. Li, H. & Durbin, R. Fast and accurate long-read alignment with Burrows–Wheeler transform. *Bioinformatics* **26**, 589–595 (2010).
49. Li, H. et al. The Sequence Alignment/Map format and SAMtools. *Bioinformatics* **25**, 2078–2079 (2009).
50. Jónsson, H., Ginolhac, A., Schubert, M., Johnson, P. L. F. & Orlando, L. mapDamage2.0: fast approximate Bayesian estimates of ancient DNA damage parameters. *Bioinformatics* **29**, 1682–1684 (2013).
51. Prüfer, K. snpAD: an ancient DNA genotype caller. *Bioinformatics* **34**, 4165–4171 (2018).
52. Green, R. E. et al. A complete Neandertal mitochondrial genome sequence determined by high-throughput sequencing. *Cell* **134**, 416–426 (2008).
53. Bolger, A. M., Lohse, M. & Usadel, B. Trimmomatic: a flexible trimmer for Illumina sequence data. *Bioinformatics* **30**, 2114–2120 (2014).
54. Li, H. Aligning sequence reads, clone sequences and assembly contigs with BWA–MEM. Preprint at https://doi.org/10.48550/arXiv.1303.3997 (2013).
55. McKenna, A. et al. The Genome Analysis Toolkit: a MapReduce framework for analyzing next-generation DNA sequencing data. *Genome Res.* **20**, 1297–1303 (2010).
56. Kumar, S., Stecher, G., Peterson, D. & Tamura, K. MEGA-CC: computing core of molecular evolutionary genetics analysis program for automated and iterative data analysis. *Bioinformatics* **28**, 2685–2686 (2012).
57. Kumar, S., Stecher, G. & Tamura, K. MEGA7: Molecular Evolutionary Genetics Analysis version 7.0 for bigger datasets. *Mol. Biol. Evol.* **33**, 1870–1874 (2016).
58. Vihtakari, M. PlotSvalbard: User Manual. *Github* https://mikkovihtakari.github.io/PlotSvalbard/articles/PlotSvalbard.html (2020).
59. Yu, G., Smith, D. K., Zhu, H., Guan, Y. & Lam, T. T. ggtree: an R package for visualization and annotation of phylogenetic trees with their covariates and other associated data. *Methods Ecol. Evol.* **8**, 28–36 (2017).
60. Yu, G. Using ggtree to visualize data on tree-like structures. *Curr. Protoc. Bioinformatics* **69**, e96 (2020).
61. Yu, G., Lam, T. T., Zhu, H. & Guan, Y. Two methods for mapping and visualizing associated data on phylogeny using ggtree. *Mol. Biol. Evol.* **35**, 3041–3043 (2018).
62. Wang, L.-G. et al. Treeio: an R package for phylogenetic tree input and output with richly annotated and associated data. *Mol. Biol. Evol.* **37**, 599–603 (2020).
63. Lindqvist, C. et al. Complete mitochondrial genome of a Pleistocene jawbone unveils the origin of polar bear. *Proc. Natl Acad. Sci. USA* **107**, 5053–5057 (2010).
64. Edgar, R. C. MUSCLE: multiple sequence alignment with high accuracy and high throughput. *Nucleic Acids Res.* **32**, 1792–1797 (2004).
65. Stamatakis, A. RAxML version 8: a tool for phylogenetic analysis and post-analysis of large phylogenies. *Bioinformatics* **30**, 1312–1313 (2014).
66. Browning, B. L. & Browning, S. R. Genotype imputation with millions of reference samples. *Am. J. Hum. Genet.* **98**, 116–126 (2016).
67. Kelleher, J., Etheridge, A. M. & McVean, G. Efficient coalescent simulation and genealogical analysis for large sample sizes. *PLoS Comput. Biol.* **12**, e1004842 (2016).
68. Palkopoulou, E. et al. Complete genomes reveal signatures of demographic and genetic declines in the woolly mammoth. *Curr. Biol.* **25**, 1395–1400 (2015).
69. Green, R. E. et al. A draft sequence of the Neandertal genome. *Science* **328**, 710–722 (2010).
70. Patterson, N. et al. Ancient admixture in human history. *Genetics* **192**, 1065–1093 (2012).
71. Vershinina, A. O. et al. Ancient horse genomes reveal the timing and extent of dispersals across the Bering Land Bridge. *Mol. Ecol.* **30**, 6144–6161 (2021).
72. Chen, L., Wolf, A. B., Fu, W., Li, L. & Akey, J. M. Identifying and interpreting apparent Neanderthal ancestry in African individuals. *Cell* **180**, 677–687.e16 (2020).
73. Quinlan, A. R. & Hall, I. M. BEDTools: a flexible suite of utilities for comparing genomic features. *Bioinformatics* **26**, 841–842 (2010).
74. Lisiecki, L. E. & Raymo, M. E. A Pliocene-Pleistocene stack of 57 globally distributed benthic $\delta^{18}O$ records. *Paleoceanography* **20**, PA1003 (2005).

Acknowledgements

We thank K. Wang and S. Schiffels for help with the MSMC-IM and MSMC analyses and E. Palkopoulou for assistance with the PSMC analysis. We thank B. Nelson for assistance with some of the Bruno extractions and the Science for Life Laboratory, Knut and Alice Wallenberg Foundation, National Genomics Infrastructure funded by the Swedish Research Council and the Uppsala Multidisciplinary Center for Advanced Computational Science for assistance with massively parallel sequencing and access to the UPPMAX computational infrastructure. L.D. acknowledges support from Formas (grant no. 2018-01640). Field support and initial funding for analysis was provided by the Arctic Field Office, Bureau of Land Management, Department of Interior, Fairbanks,

Alaska, USA. This work was supported in part by National Science Foundation Division of Environmental Biology grant no. 1754451 to B.S.

Author contributions

D.M., P.G. and M.K. discovered and excavated Bruno from the field site. B.S. and R.E.G. designed the research project and supervised the analysis. M.-S.W. and R.E.G. performed the analysis, with contributions from R.C.-D. and G.G.R.M. J.D.K. performed the extraction of ancient DNA and prepared the sequencing library. L.D. coordinated the genome sequencing and edited the manuscript. B.S., M.-S.W., G.G.R.M., I.S. and R.E.G. drafted the manuscript. A.O.V., M.A.S., S.E.C. and P.G. improved the figures and supplementary material. K.L.L. contributed the genomes for modern polar bears. All authors contributed to the final manuscript.

Competing interests

The authors declare no competing interests.

Additional information

Extended data is available for this paper at https://doi.org/10.1038/s41559-022-01753-8.

Supplementary information The online version contains supplementary material available at https://doi.org/10.1038/s41559-022-01753-8.

Correspondence and requests for materials should be addressed to Beth Shapiro.

Peer review information *Nature Ecology & Evolution* thanks Choongwon Jeong and the other, anonymous, reviewer(s) for their contribution to the peer review of this work. Peer reviewer reports are available.

Reprints and permissions information is available at www.nature.com/reprints.

Publisher's note Springer Nature remains neutral with regard to jurisdictional claims in published maps and institutional affiliations.

Extended Data Fig. 1 | Images of Bruno's skull. Images of Bruno's skull. (a) ventral, (b) lateral, (c) dorsal views, and (d) shown along with a brown bear skull (left) and a mature polar bear skull (right). Photos by Pam Groves.

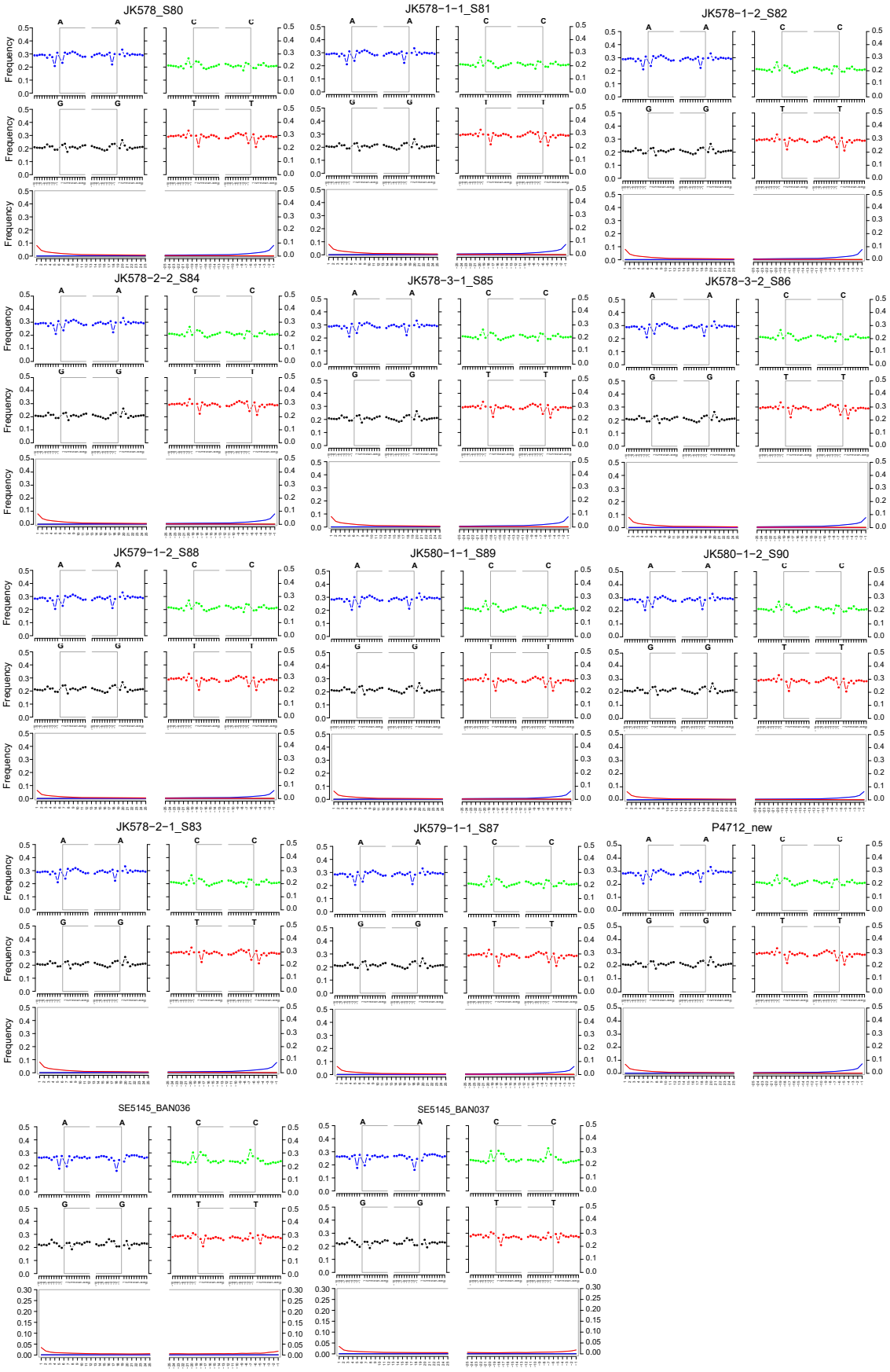

Extended Data Fig. 2 | MapDamage plot for each of the 14 sequencing libraries prepared from DNA extracts from Bruno. MapDamage plot for each of the 14 sequencing libraries prepared from DNA extracts from Bruno. Plots show the frequency of C>T and G>A substitutions. SE5145_BAN036 and SE5145_BAN037 are single-stranded DNA libraries and appear to have less damage than the other libraries.

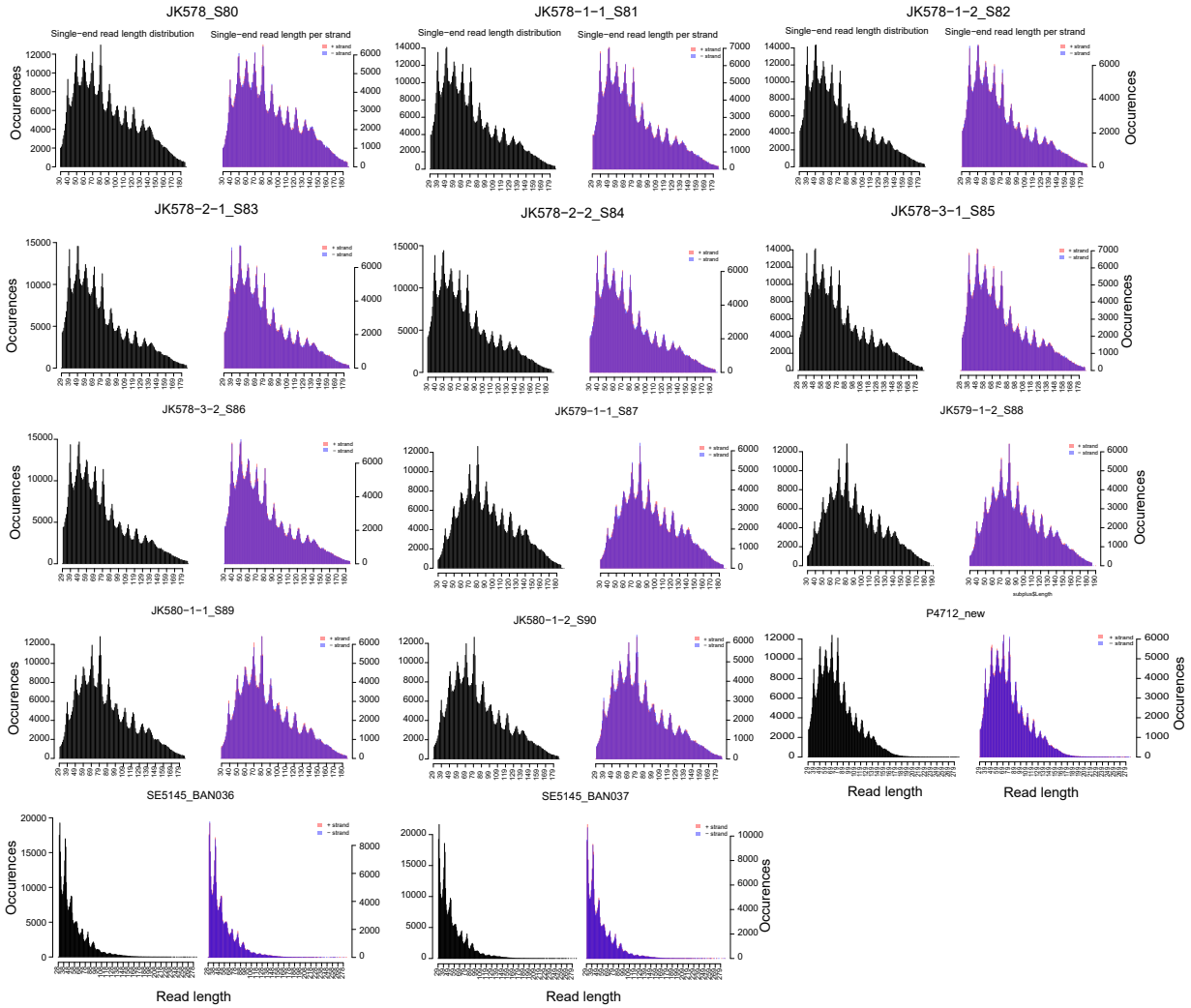

Extended Data Fig. 3 | An example of read length distributions for each of the 14 DNA sequencing libraries prepared from DNA extracts from Bruno. An example of read length distributions for each of the 14 DNA sequencing libraries prepared from DNA extracts from Bruno. The observed ~10 bp periodicity of recovered fragment lengths is commonly observed in nuclear DNA recovered from old tissues and is most likely explained by nucleosomal protection of DNA molecules.

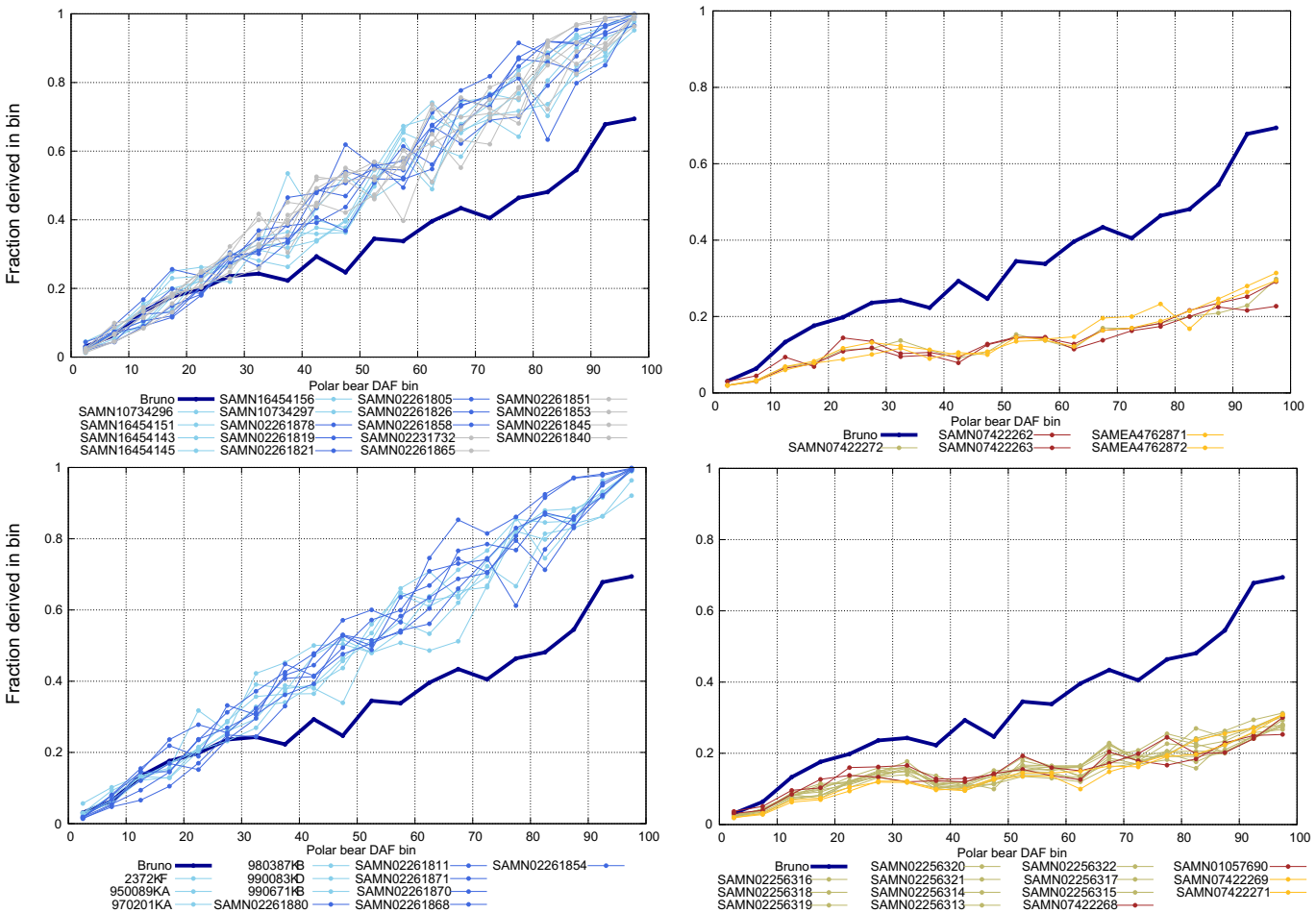

Extended Data Fig. 4 | The derived allele frequencies of polar bears, brown bears, and Bruno at polar bear polymorphic sites. The derived allele frequencies of polar bears, brown bears, and Bruno at polar bear polymorphic sites. We measured the derived allele frequency for all sites observed to be segregating polymorphism in the polar bears in the panel. For each 5% frequency bin, we measured the observed derived allele frequency within each polar bear (left panels) and each brown bear (right panels). The Bruno bear is in each panel (thick blue line). As expected, each polar bear carries the derived allele as often as would be expected given the derived allele frequency within polar bears (red, x = y line). Brown bears carry far fewer polar bear derived alleles. Genetically, Bruno is clearly not a modern polar bear nor a brown bear. An American black bear genome was used to polarize the ancestral state of alleles. Seven brown bears (SAMN07422261, SAMN07422264, SAMN07422265, SAMN07422266, SAMEA4762870, SAMN07422267, and SAMN07422270) were excluded from this analysis due to low sequencing coverage.

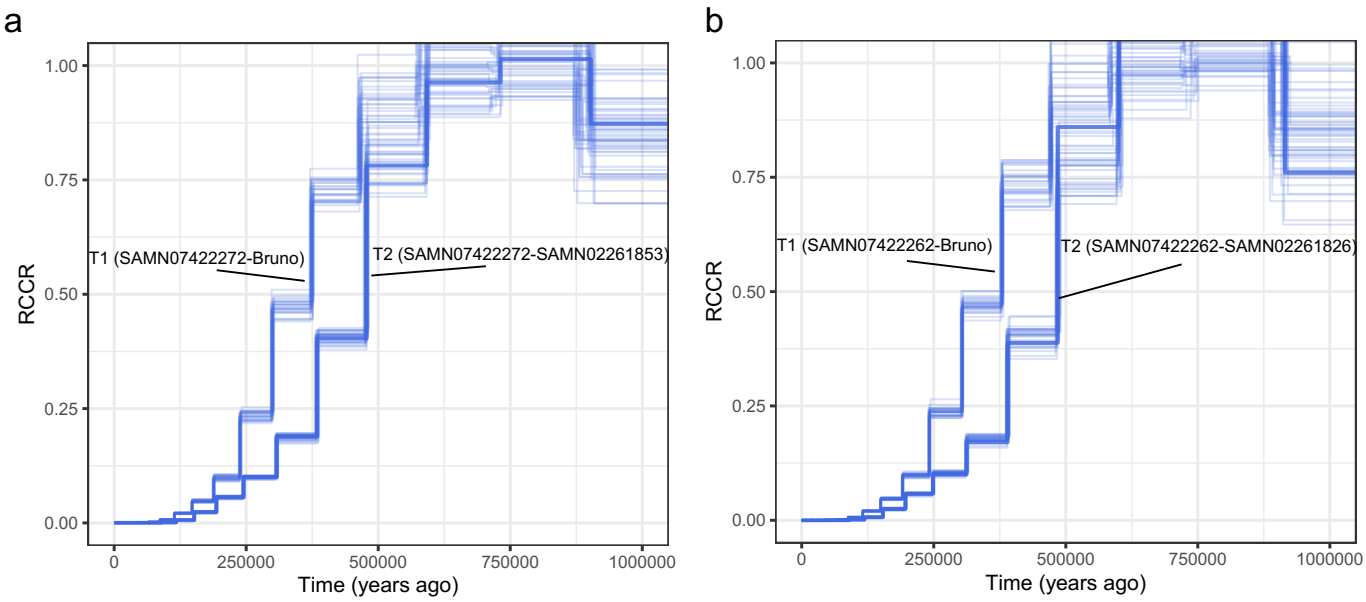

Extended Data Fig. 5 | MSMC estimates the relative cross coalescence rate (RCCR) and divergence time between Bruno and an extant brown bear and between extant polar bear and the same brown bear. MSMC estimates the relative cross coalescence rate (RCCR) and divergence time between Bruno and an extant brown bear and between extant polar bear and the same brown bear. Two independent analyses using different polar bears (IDs: SAMN02261853 and SAMN02261826) and brown bears (IDs: SAMN07422272 and SAMN07422262) are shown as A and B. For each calculation, we performed 30 bootstrap replicates, which are shown as thin red lines. Based on a 50% RCCR, we estimate the divergence time for modern polar bears and brown bears (T2) to be 481,049 ± 4500 (mean ± SD) years ago, which is consistent with previous estimates (Liu et al. 2014), and the divergence time for Bruno and brown bears (T1) to be 376.9 ± 3.3 kya (mean ± SD). The resulting estimate for the time difference between when Bruno and the modern polar bear diverged from the brown bear (a rough estimate of how long ago Bruno died) is: $\Delta T = T2\text{-}T1 = 104.4 \pm 3.4$ kya.

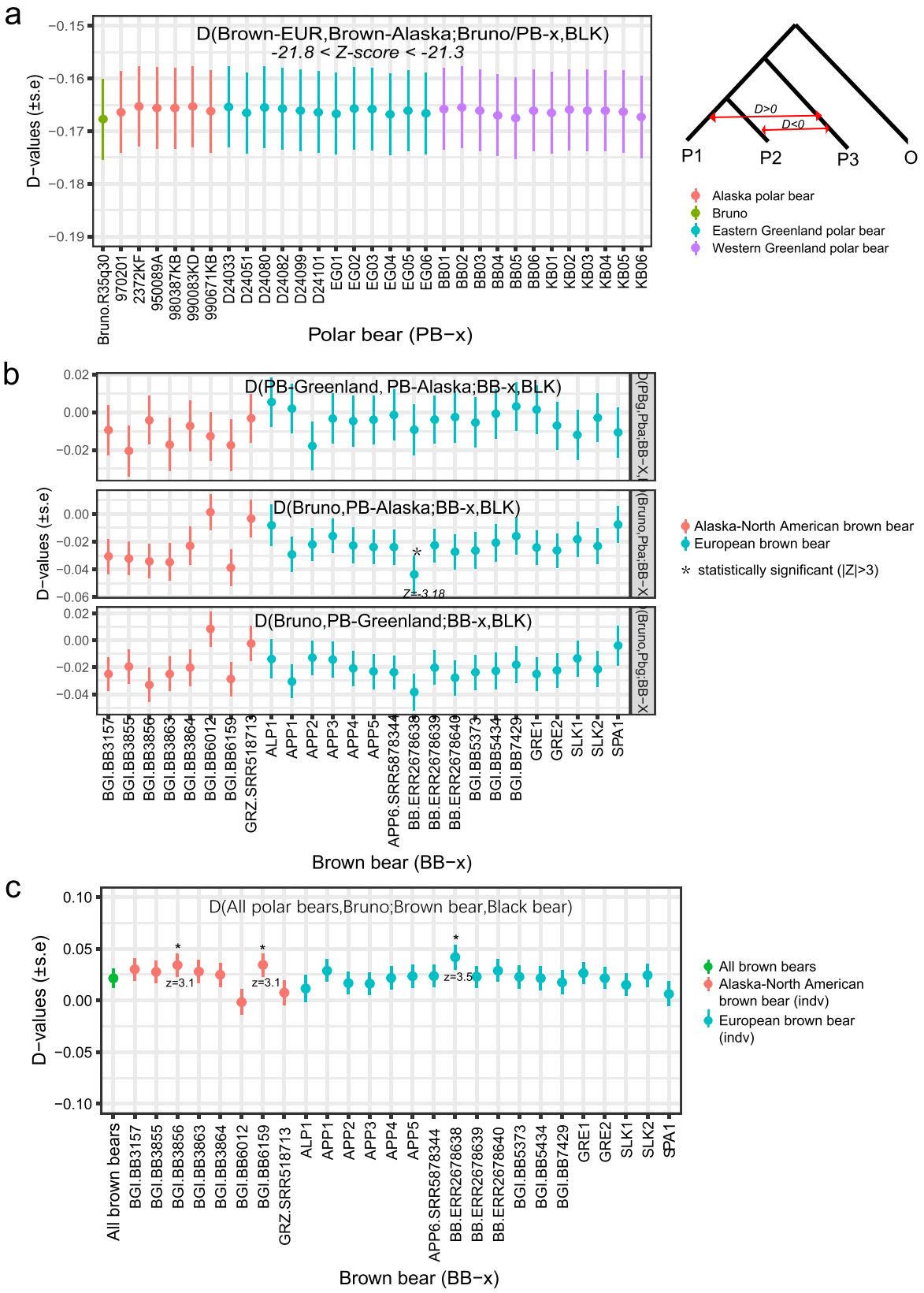

Extended Data Fig. 6 | D-statistics analysis of gene flow between polar bears and brown bears. D-statistics analysis of gene flow between polar bears and brown bears. (a) D-statistics in the form of D(brown bear-Europe; brown bear-N America; Bruno/Polar bear, Black bear). All combinations give significant negative values (−21.8 < Z-score < −21.3), suggesting admixture occurred between polar bears and North American brown bears, consistent with previous work. (b) D-statistics in the forms of D(PB-Greenland,PB-Alaska;BB-x,BLK), D(Bruno,PB-Alaska;BB-x,BLK) and D(Bruno,PB-Greenland; BB-x,BLK) are mostly non-significant (−3 < Z-score < 3). (c) Results of D-statistics in the form of D(All polar bears,Bruno;Brown bear,BLK).

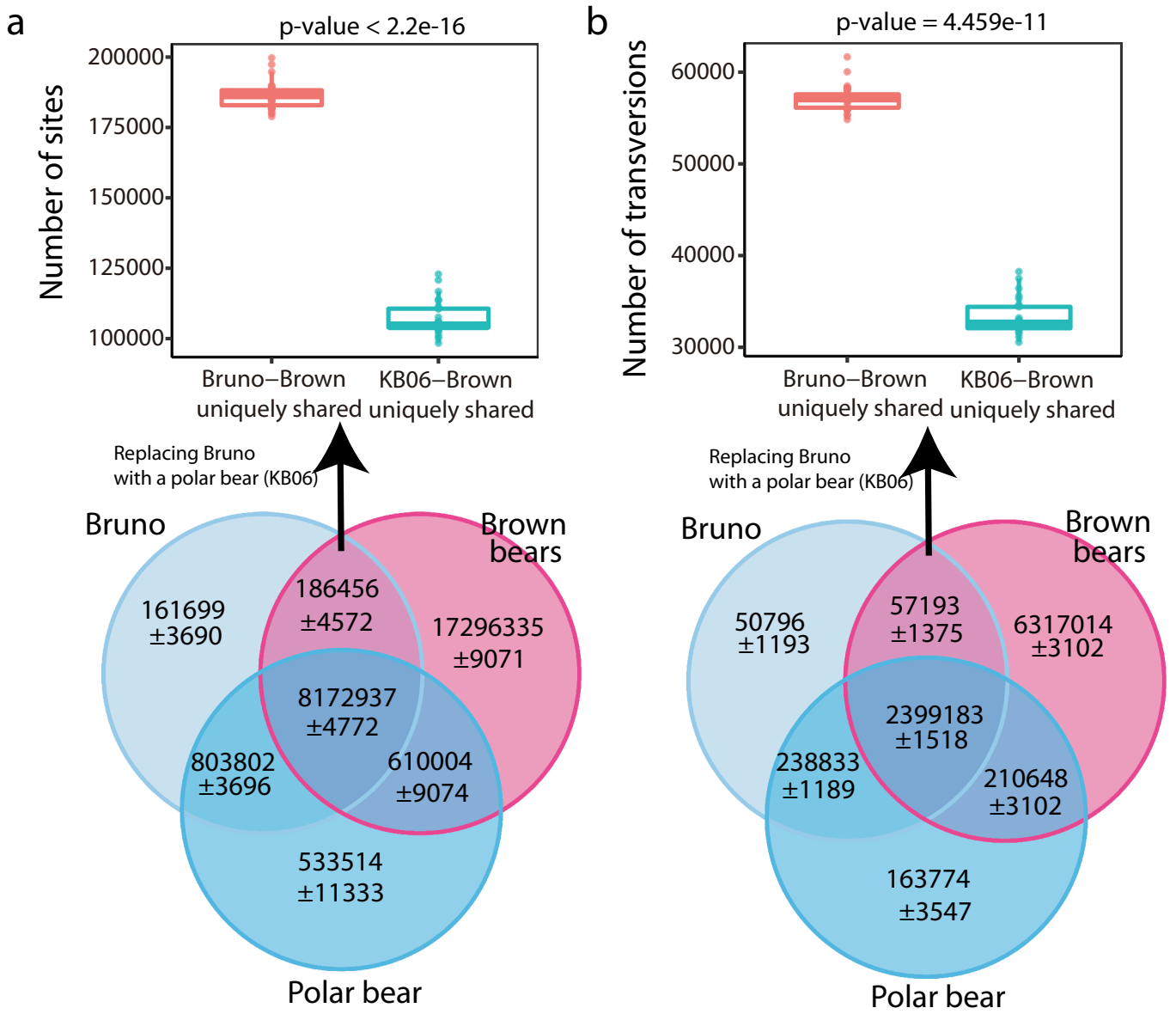

Extended Data Fig. 7 | Allele sharing among Bruno, all brown bears, and a polar bear. Allele sharing among Bruno, all brown bears, and a polar bear. (a) and (b) show the shared derived alleles (transversions+transitions) and transversions, respectively. Replacing data from Bruno with data from an extant polar bear, KB06, results in fewer alleles shared uniquely with all brown bears to the exclusion of other polar bears. Statistical significance was measured by the wilcox.test (two-sided) using R version 4.10.

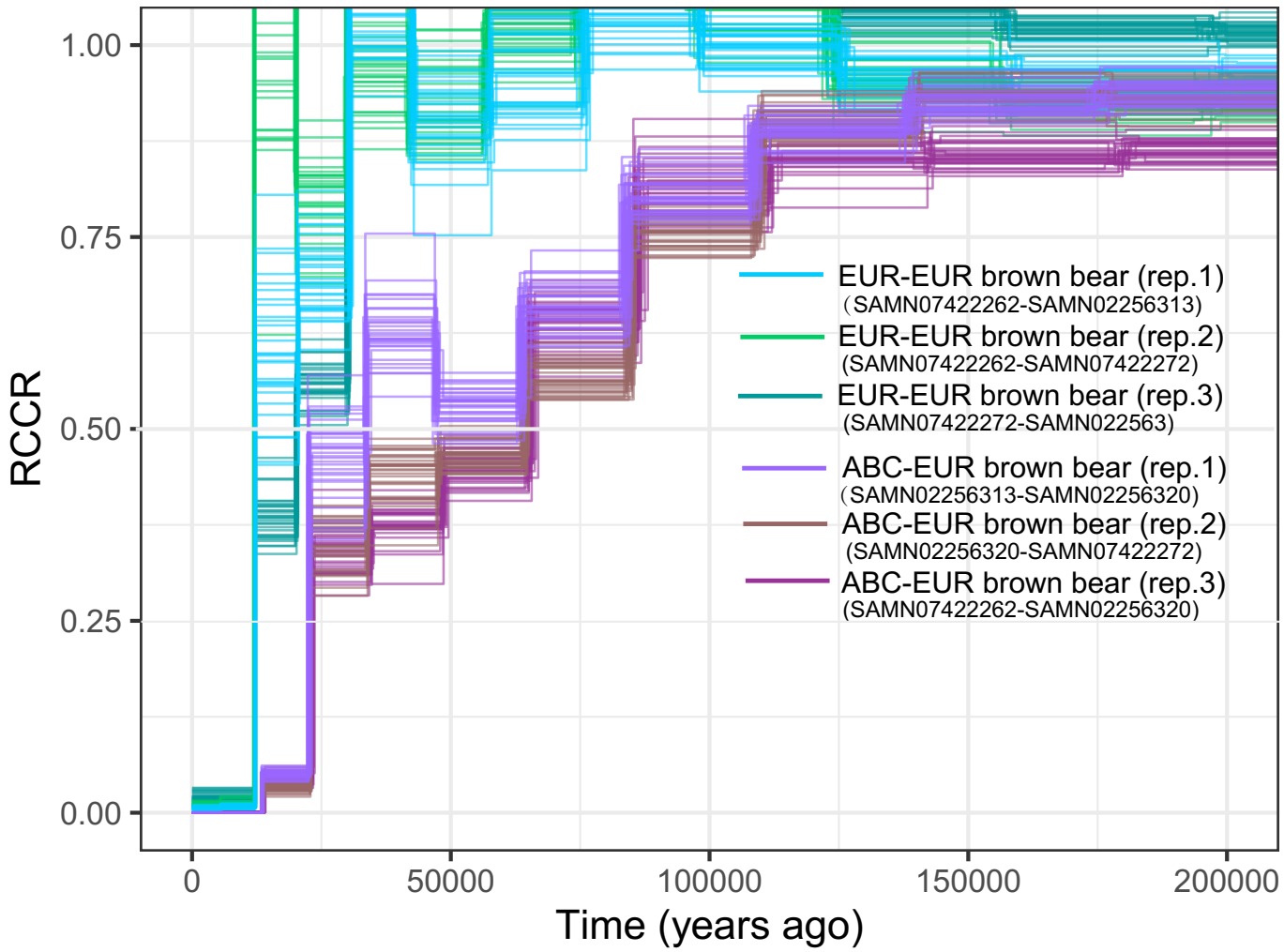

Extended Data Fig. 8 | MSMC estimates the relative cross coalescence rate (RCCR) and divergence time between brown bears. MSMC estimates the relative cross coalescence rate (RCCR) and divergence time between brown bears. Three independent analyses were performed for each pair. Based on a 50% RCCR, divergence time for North American and European Brown bears is 23–65 kya, which is more recent than the death of Bruno. We note that polar bear ancestry in North American bear genomes may affect these MSMC estimates and therefore perform DFOIL in multiple configurations that assume both a more recent and more ancient divergence between North American and European brown bears than the age of Bruno.

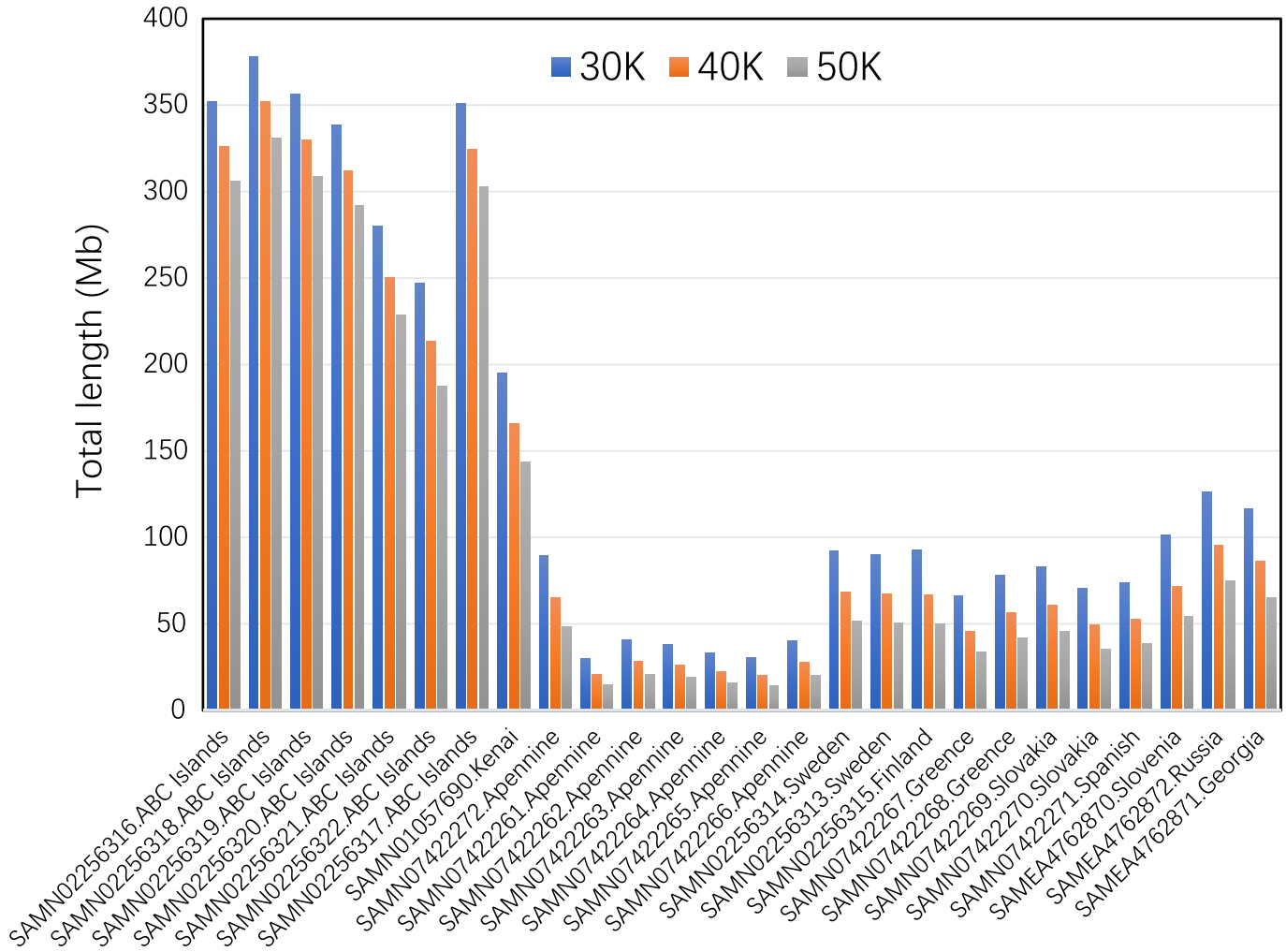

Extended Data Fig. 9 | IBDMix inferred the amount of the genome showing a signal of admixture between Bruno and brown bears. IBDMix inferred the amount of the genome showing a signal of admixture between Bruno and brown bears. Blue, orange and gray lines show results when the minimum lengths of 30 kb, 40 kb and 50 kb were used as cut-off to recover admixed regions.

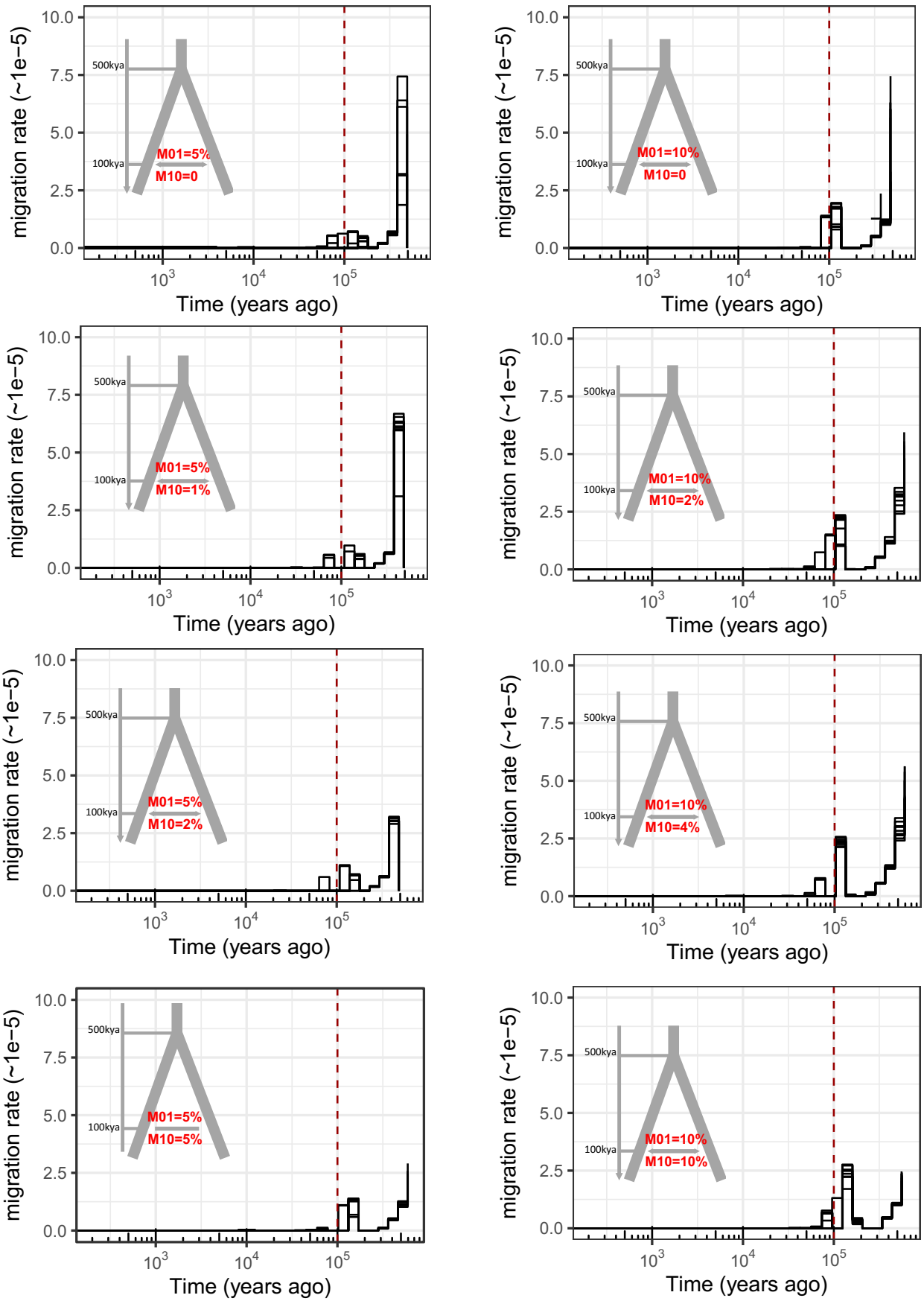

Extended Data Fig. 10 | See next page for caption.

Extended Data Fig. 10 | Analysis of simulated data shows that MSMC-IM is robust to the directionality of gene flow is robust. Analysis of simulated data shows that MSMC-IM is robust to the directionality of gene flow is robust. We assumed eight scenarios in which two populations diverged 500 kya with asymmetrical and symmetrical migrations at 100 kya, as described in Methods. Labeling is as follows: 'M01 = 5%' indicates that pop0 contributed 5% ancestry to pop1, 'M10 = 5%' indicates that pop1 contributed 5% ancestry to pop0. Vertical red dashed lines show the time of migration at 100 kya. Models and magnitude of migration for each direction are shown within each plot.

nature portfolio

Corresponding author(s): Beth Shapiro

Last updated by author(s): Mar 18, 2022

Reporting Summary

Nature Portfolio wishes to improve the reproducibility of the work that we publish. This form provides structure for consistency and transparency in reporting. For further information on Nature Portfolio policies, see our Editorial Policies and the Editorial Policy Checklist.

Statistics

For all statistical analyses, confirm that the following items are present in the figure legend, table legend, main text, or Methods section.

n/a	Confirmed
☐	☒ The exact sample size (*n*) for each experimental group/condition, given as a discrete number and unit of measurement
☐	☒ A statement on whether measurements were taken from distinct samples or whether the same sample was measured repeatedly
☐	☒ The statistical test(s) used AND whether they are one- or two-sided *Only common tests should be described solely by name; describe more complex techniques in the Methods section.*
☒	☐ A description of all covariates tested
☐	☒ A description of any assumptions or corrections, such as tests of normality and adjustment for multiple comparisons
☐	☒ A full description of the statistical parameters including central tendency (e.g. means) or other basic estimates (e.g. regression coefficient) AND variation (e.g. standard deviation) or associated estimates of uncertainty (e.g. confidence intervals)
☐	☒ For null hypothesis testing, the test statistic (e.g. *F*, *t*, *r*) with confidence intervals, effect sizes, degrees of freedom and *P* value noted *Give P values as exact values whenever suitable.*
☒	☐ For Bayesian analysis, information on the choice of priors and Markov chain Monte Carlo settings
☒	☐ For hierarchical and complex designs, identification of the appropriate level for tests and full reporting of outcomes
☒	☐ Estimates of effect sizes (e.g. Cohen's *d*, Pearson's *r*), indicating how they were calculated

Our web collection on statistics for biologists contains articles on many of the points above.

Software and code

Policy information about availability of computer code

Data collection	SeqPrep2, bwa v0.7.12-r1039, MapDamage v2.0.6-2-g6507525, SAMtools v0.1.19, snpAD v0.3.4, VCFtools v0.1.5, MIA v1.0, Trimmomatic v0.39, GATK v3.7.0, BCFtools v1.4-7-g41827a3-dirty
Data analysis	MEGA7, R, PlotSvalbard, ggtree, treeio, PSMC v0.6.5-r67, MSMC2, MUSCLE v3.8.31, RAxML v8.1.17, Figtree v1.3.1, BEAGLE v4.1, SNPable toolkit, MSMC-IM, AdmixTools (qpDstat), DFOIL, BEDTools v2.25.0

For manuscripts utilizing custom algorithms or software that are central to the research but not yet described in published literature, software must be made available to editors and reviewers. We strongly encourage code deposition in a community repository (e.g. GitHub). See the Nature Portfolio guidelines for submitting code & software for further information.

Data

Policy information about availability of data

All manuscripts must include a data availability statement. This statement should provide the following information, where applicable:

- Accession codes, unique identifiers, or web links for publicly available datasets
- A description of any restrictions on data availability
- For clinical datasets or third party data, please ensure that the statement adheres to our policy

Raw sequencing reads generated in our study are available from the NCBI Sequence Read Archive (SRA) Bio-project accession: PRJNA720153.

Field-specific reporting

Please select the one below that is the best fit for your research. If you are not sure, read the appropriate sections before making your selection.

☒ Life sciences ☐ Behavioural & social sciences ☐ Ecological, evolutionary & environmental sciences

For a reference copy of the document with all sections, see nature.com/documents/nr-reporting-summary-flat.pdf

Life sciences study design

All studies must disclose on these points even when the disclosure is negative.

Sample size	No statistical method was used to determine the ancient sample size as a priori in this study.
Data exclusions	No data was excluded.
Replication	Only one high-coverage ancient genome was sequenced in this study.
Randomization	No randomization was performed as only one ancient sample was included in this study
Blinding	This data was not grouped for analysis. No blinding was applied.

Reporting for specific materials, systems and methods

We require information from authors about some types of materials, experimental systems and methods used in many studies. Here, indicate whether each material, system or method listed is relevant to your study. If you are not sure if a list item applies to your research, read the appropriate section before selecting a response.

Materials & experimental systems

n/a	Involved in the study
☒	☐ Antibodies
☒	☐ Eukaryotic cell lines
☐	☒ Palaeontology and archaeology
☒	☐ Animals and other organisms
☒	☐ Human research participants
☒	☐ Clinical data
☒	☐ Dual use research of concern

Methods

n/a	Involved in the study
☒	☐ ChIP-seq
☒	☐ Flow cytometry
☒	☐ MRI-based neuroimaging

Palaeontology and Archaeology

Specimen provenance	The Bruno skull sample was provided by University of Alaska Museum under cooperation.
Specimen deposition	The Bruno skull is housed at the University of Alaska Museum: UAMES 29513
Dating methods	Three AMS 14C dates obtained on ultrafiltered collagen extractions of bone all yielded non-finite ages (Beta-283240: >43,500 14C; OxA-23894: >50,500 14C; OxA-23986: >50,500 14C). We dated the age of Bruno using genetic method.

☒ Tick this box to confirm that the raw and calibrated dates are available in the paper or in Supplementary Information.

Ethics oversight	Permission to sample the fossil (the museum accession number: UAMES 29513) was granted by the University of Alaska Museum of the North

Note that full information on the approval of the study protocol must also be provided in the manuscript.